

**Ministry of Higher Education and Scientific Research
University of Baghdad
Institute of Laser for Postgraduate Studies**



Quantum Repeaters Based on Multiplexed Single-Photon Source

**A Thesis Submitted to the Institute of Laser
for Postgraduate Studies, University of
Baghdad in Partial Fulfillment of the
Requirements for the Degree of Master of
Science in Laser / Electronic and
Communication Engineering**

**By
Wijdan Mahmood Khudhair**

B.Sc. Communications Engineering – 2007

**Supervisor
Lecturer. Dr. Jawad A.K Hasan**

Dedication

***To express my gratitude to those who supported and
Give me the inspiration, I dedicate this dissertation***

To

.... Allah

Then, to My Self.....

And To

The Beloved Heart ... My Husband "Ehab"

The PureHearts My Little Angels" Rand, Ali and Yazan"

***The Big Hearts ... My Brother"Maher" and My
Sisters" Eman, Hanan and Marwa"***

***The White Heatrs ... My friends who encourage and
support me.***

The Great Iraqi martyrs.

Wijdan

Acknowledgment

I would like to express my deep gratitude and appreciation to my inspiration source and energetic supervisor, who suggested this work, **Dr. Jawad A.K Hasan** for his advice, guidance, helpful suggestion, encouragement and his expensive time that he gave during this work.

Great appreciation is to **Prof. Dr. Abdul Hadi M. Al-Janabi**, Dean of the Institute of Laser for Postgraduate Studies, for his encouragement, help, and his support during my research work.

Great respect is to **Asst. Prof. Dr. Mohammed K. Thaher**, Asst. Dean of the Institute of Laser for Postgraduate Studies, for his support and advices.

Appreciation is to **Asst. Prof. Dr. Ziyad Ayad Taha**, head of the Engineering and Industrial Applications Dept. for his cooperation to proceed with this work.

Also, many thanks go to **Asst. Prof. Dr. Hussein A. Jawad**, for his guidance and support.

Great appreciation is to **Asst. Prof. Dr. Tahreer Safaa Mansour**, for her continuous support and help during my research work.

Appreciation is to **Asst. Prof. Dr. Fadil A. Omran**, for his cooperation and support to proceed with this work.

Finally, Great thanks to my colleagues **Ra'ad S. Abood, Raghad S. Hasan, Adnan N. Kadhim, Yousif I. Hammadi, Ibrahim L. Abdul Jabbar, Alaa J. Jumaah, Sura H. Mahmood, Aya T. Yahea, Dhuha N. Issa, Akram S. Ahmed, Ameen Waleed and Abd alstaar Maa'n.**

Wijdan Mahmood Khudhair

Abstract

The transmission of any quantum information over long distances with less errors is restricted by the exponential decay of light transmission with the length of the optical fiber. Hence, to overcome this issue, the quantum repeater was suggested by Briegel in 1998. The main goal of the implementation of the quantum repeater is to distribute the entangled photons between the sender and the receiver. The quantum repeater ingredients are the quantum memory, Bell state measurement and entangled photon sources. There are many of quantum repeater schemes was proposed, some used photon pair source. Photon pair source suffers from error mechanism related with photon emission and transmission probability of loss and so reduces the entanglement distribution rate. Other quantum repeater scheme proposed used single photon source which have less error than photon pair source suffered from, so the entanglement distribution rate could be improved.

The most important parts in the quantum repeater are the quantum memory and the entangled photon source. In case of quantum memory, multiplexed multimode quantum memories are proposed. The governed parameter in quantum memory is its lifetime. Our calculations, show that the short lifetime quantum memories show more overall entanglement distribution rate than the long lifetime quantum memories.

A quantum repeater scheme based on multiplexed photon pair source was suggested in this work and the results shows slightly improving of entanglement distribution rate comparing with quantum repeater scheme based on photon pair source.

On the other side, a comparison study about entanglement distribution rate of photon pair source and single photon source was done.

For more improvement in entanglement distribution over long distance quantum communications, an efficient architecture for quantum repeaters based on multiplexing single-photon sources in combination with multiplexing multimode quantum memories was also suggested here, to increase the entanglement between arbitrary photon number of remote quantum memories. The calculation of single photon source parameters illustrates the improvement in the entire entanglement distribution rate. In this work, a simulation study was carried out using the Python 3.7 simulation software.

Contents

Subject	Page no.
Abstract	I
List of abbreviations	Iii
List of symbols	Iv
Chapter one: Introduction and Basic Concepts	
1.1 Introduction	1
1.2 Aim of The Work	4
1.3 Fundamentals of Quantum Mechanics	4
1.3.1 Dirac Notation and The Quantum State	6
1.3.2 Linear Algebra and The Operators	8
1.3.3 The Density Operator	10
1.3.4 The Postulates of Quantum Mechanics	13
1.4 The Quantum Computing	15
1.4.1 Quantum bit (Qubit)	16
1.4.2 Quantum Entanglement	20
1.5 The Quantum Gates	21
1.5.1 Single-input gates	22
1.5.2 Two-input gates	24
1.6 Quantum Communication	27
1.6.1 Advantages of Quantum Communication vs. Classical Communication	32
1.6.2 The Direct Transmission (point to point)	33
1.6.3 The Quantum no-Cloning Theorem	34
1.6.4 The Quantum Repeater QR	34
1.6.5 The Ingredients of Quantum Repeater	35
1.6.5.1 The Quantum Memories QMs	35
1.6.5.2 Bell State Measurement BSM	36
1.6.5.3 Quantum Teleportation and Entanglement Swapping	36
1.6.5.4 The Entangled Photon Sources	37
1.6.5.4.1 The QR Scheme Based on Photon Pair Source	37
1.6.5.4.2 The QR Scheme Based on Single Photon Source	40
1.6.5.4.3 Multiplexed Single Photon Source	44
1.6.5.4.4 Multimode Quantum memories MM-QMs	46
1.7 Literature Survey	49
Chapter two: Simulation Works	
2.1 The Simulation Works	53
2.2 The performance of The Short Lifetime MM-QMs -QR	53

2.3	A Comparison Study for the Performance of QR Based on PPS and QR Based on SPS	54
2.4	The New Approachs to Re-design a quantum repeater	55
2.4.1	New Design of The QR Scheme Based on Multiplexed Photon pair Source	55
2.4.2	New Design of The QR Scheme Based on Multiplexed Single Photon Source	57
Chapter three: Results, Discussion, Conclusions and Future work		
3.1	Introduction	60
3.2	The Relationship of Lifetime MM-QM with Entanglement Rate	60
3.3	The Entanglement Distribution Rate of QR Scheme Based on MUX-PPS	63
3.4	The Entanglement Distribution Rate of QR Schemes Based on SPS and PPS	63
3.5	The Entanglement Distribution Rate of QR Scheme Based on MUX-SPS	65
3.6	Discussion	67
3.7	Conclusions	67
3.8	Future work	69
	References	70

List of Abbreviations

AFC	Atomic frequency comb
BS	Bell states
BSM	Bell states measurement
CNOT	Controlled NOT gate
DSF	Dispersion shifted fibers
DLCZ	Duan–Lukin–Cirac–Zoller
EIT	Electromagnetically-induced transparency
FWM	Four wave mixing
HSPS	Heralded single-photon source
MM-QM	Multimode quantum memory
MUX-PPS	Multiplexed Photon pair source
MUX-SPS	Multiplexed Single photon source
NRD	Number-resolving detector
PCF	Photonic crystal fibers
PPS	Photon pair source
PLOB	Pirandola, Laurenza, Ottaviani, and Banchi
QD	Quantum dot
QKD	Quantum key distribution
Qubit	Quantum bit
QR	Quantum repeater
QM	Quantum memory
SPDC	Spontaneous parametric down conversion
SRS	Spontaneous Raman scattering
SFWM	Spontaneous four wave mixing
SWAP	swapping gate
SPS	Single photon source
SPD	Single-photon detector
TGW	Takeoka, Guha, and Wilde
TD	Threshold detector

List of Symbols

Symbol	Meaning
B	Total bandwidth of OM
β	The beam splitter transmission coefficient
\mathbb{C}	Complex number
$\langle f_{\tau,m} \rangle$	Entanglement swapping rate
H	Hilbert space
\mathcal{H}	Hermitian operator
\hbar	Reduced Planck constant
I	Identity operator
L	Total distance between sender and receiver
L_{att}	Attenuation length
L_0	Elementary link length
M_m	Measurement operators
m	Quantum memory mode number
n	Elementary link number
P_0	Entanglement creation probability
P_1	Entanglement swapping probability
$P_{success}$	Probability of success of entanglement generation
P_m	Projective Measurement
$R_{success}$	Entanglement distribution rate
R_{PLOB}	PLOB bound (key rate)
R_{TGW}	TGW bound (key rate)
r_m	Measurement outcome
τ	Quantum memory lifetime
tr	Trace of a matrix
U	Unitary operator
$U(\Delta t)$	Time evolution operator
V	Vector space
w	Bandwidth inefficiency of OM
\otimes	Tensor product
$ \xi ^2$	Squeezing parameter of the laser source
η	Transmissivity

η_i	The idler arm efficiency
η_s	The overall transmission on the signal arm efficiency
η_{mem}	Quantum memory efficiency
ρ	Density operator
ρ^2	The probability of PPS to emit photons

List of Figures

Fig. No.	Title of Figures	Page
Fig. (1.1)	The representation of qubit on Bloch sphere	18
Fig. (1.2)	A qubit as a photon (a particle of light) travelling along two possible paths when a photon encounters a beam splitter	20
Fig. (1.3)	The CNOT gate.	23
Fig. (1.4)	The Swap gate.	26
Fig. (1.5)	Quantum teleportation sceme. A qubit (quantum state) transmitted from one location to another.	28
Fig. (1.6)	Quantum teleportation performing steps.	29
Fig. (1.7)	A quantum repeater scheme. Dots represent quantum memories, lines show entanglement, and dashed boxes indicate Bell state measurements	31
Fig. (1.8)	A quantum repeater scheme implements steps.	32
Fig. (1.9)	Bell State Measurement BSM. The bar is 50:50 beam splitter BS, D_1 and D_2 are detectors.	36
Fig. (1.10)	The single photon source experimental setup.	37

Fig. (1.11)	Scheme of a quantum repeater based on multiplexing Multimode quantum memory MM-QM and photon pair source PPS.	38
Fig. (1.12)	Scheme of a quantum repeater using single photon source SPS.	41
Fig. (1.13)	The MUX-SPS scheme.	44
Fig. (1.14)	(a) Quantum repeater scheme. (b) Multiplexing multimode quantum memory MM-QM.	47
Fig. (2.1)	Multiplexed photon pair source MUX-PPS.	56
Fig. (2.2)	Scheme of a quantum repeater using multiplexed photon pair source MUX-PPS-QR protocol.	56
Fig. (2.3)	Suggested scheme of QR uses MM-QM in combination with MUX-SPS. Bars represent Beam splitter BS.	58
Fig. (3.1)	The entanglement distribution rate of MM-QMs with different QM times.	60
Fig. (3.2)	The entanglement distribution rate of QR scheme based on MUX-PPS. (Blue line) of PPS, (Dashed line) of MUX-PPS.	63
Fig. (3.3)	The entanglement distribution rate of QR scheme based on SPS. (Red line) of SPS, (Blue line) of PPS.	64
Fig. (3.4)	The entanglement distribution rate of QR scheme based on MUX-SPS and SPS. (Dashed line) of MUX-SPS, (Red line) of SPS.	65
Fig. (3.5)	The entanglement distribution rate of QR scheme based on MUX-SPS. (Blue line) of	66

	MUX-SPS with NPD, (Dashed line) of MUX-SPS with TD, (Red line) of SPS.	
--	--	--

List of Tables

Table No.	Title of Tables	Page
Table (1.1)	Dirac notation.	6
Table (1.2)	Truth table of CNOT gate.	24
Table (1.3)	Truth Table of Swap gate.	26
Table (1.4)	Bob's Pauli correctional operation on his qubit, depending on the Bell state measurement outcome.	30
Table (2.1)	Summary of different quantum memory types.	53
Table (2.2)	The differences between PPS and SPS.	54
Table (2.3)	Parameters description of SPS and PPS quantum repeaters.	55
Table (2.4)	The parameter of QR based on MUX-PPS.	57
Table (2.5)	The parameter of QR Scheme Based on MUX-SPS.	59
Table (3.1)	The entanglement distribution rate values with different quantum memories lifetime τ and different numbers of modes m	62
Table (3.2)	The entanglement distribution rate comparison results between PPS-QR and SPS-QR.	64
Table (3.3)	The entanglement distribution rate comparison results between SPS-QR and MUX-SPS-QR.	65
Table (3.4)	The entanglement distribution rate comparison results between SPS-QR and MUX-SPS-QR.	66

Chapter One

Introduction and Basic

Concepts

1.1 Introduction

Quantum communication aims at harnessing quantum mechanics concepts to develop systems that can provide a studied improvement in information processing, communication efficiency and security. The process begins by encoding the information into quantum states, storing, sending, and detecting this information using quantum techniques. As a consequence, it is possible to perform tasks within quantum communications that are simply impossible with classical communication systems because of the difference in the notion of the quantum systems and the classical systems [1].

Unfortunately, both quantum and classical data transmitted for long distances over optical fibers decays exponentially. In classical communication, data can be amplified at midway stations, keeping the signal from terminating to exist and therefore expanding the rate of transmission. In meantime, the amplification of quantum state is limited by no-cloning theorem, which prevents producing similar copies of a single unidentified quantum states [2].

The current advances in the quantum field have delivered many inventions and a significant number of these advancements are still in their earliest stages. But some of these quantum advances such quantum key distribution QKD [3], that is established between two points (point to point), have just been marketed. QKD faces a threatening problem with the long distance communications which has not been implemented except some of current records on the request of a couple of hundred kilometers because of photon loss limitation [4].

Most important features that distinct the quantum computation is the coherent superposition of quantum state $|\varphi\rangle = \alpha |0\rangle + \beta |1\rangle$; $\alpha, \beta \in \mathbb{C}$, where $|\alpha|^2 + |\beta|^2 = 1$ and \mathbb{C} is complex number. However, the quantum

state could be transmitted through the quantum teleportation protocol [5]. The quantum teleportation is a process that allow to transmit an unknown quantum state such as a photon emitted from the laser source, from one location to another (Alice and Bob) with assistance of classical communication and earlier mutual quantum entanglement between the transmitting and receiving location. A quantum state in the quantum teleportation protocol, is primarily stored in a system (e.g. A) and could be recovered at a different system (e.g. B), without having any physical movement between these two systems. The quantum teleportation principle is based on the non-local correlations, or the quantum entanglement. The quantum communications and quantum computation both use the quantum entanglement as a necessary resource. Quantum entanglement is based on quantum correlations between multiple systems, that have no distinct separable properties. Entanglement has been observed experimentally using many different systems such as, photons [6], atomic ions [7], superconducting junctions [8], atoms in cavities and an optical lattice [9, 10].

Furthermore, entanglement represents the counter-native illustration of nature projected by quantum physics, that tolerates for understandable experimental tests of quantum theory, to look like more beneficial for quantum communication and quantum computation. Photons can rapidly cross the distance between positions with simply insignificant perturbations to the encoded quantum information, so they are an accepted choice as a qubit for communications purposes [11].

At present, a chain of pioneering most important experiments include QKD and point to piont communications, have utilized photons in quantum communication protocols through distance of 144 km. But, point to piont communication of quantum information via long distances is delayed by the attenuation of light traveling through the optical fiber [12].

Thus to solve the problems which include loss of photons and the inability to copy the quantum bit (Qubit) because of the no-cloning theorem, that cannot be solved by the typical model of a repeater which does not have the ability to transfer the quantum information, it is conceivable to build quantum repeaters (QRs) to expand the transmission rate without amplifying the signals [13-19]. The essential thought of most QR schemes is to divide the total channel into (n) channel segments called elementary links, between each two elementary links there is one node. Generally, the photon transmission rate scales linearly with transmittivity η , while separating the channel to different connections will allow the photon transmission rate to scale exponentially as $\eta^{\frac{1}{n}}$. The QR nodes will connect with each other by entanglement swapping [20]. The distance between endpoints of the entire channel which is divided into a chain of elementary links and nodes can be connected by optical fibres with each other, at each node present two quantum memories (QMs), Bell state measurement (BSM) and entangled photon sources [21].

Then, entanglement can be established between pairs of nodes, and successive elementary links related through entanglement swapping, that is utilized to extend the entanglement via the total length of the QR with entanglement distribution rate limited by photon loss problem found in QMs and entangled photon sources. So as to synchronize the various stages of the quantum communication line, laser pulses are needed to store and retrieve the quantum information on demand and so QMs are used in the implementation of the nodes of the QR. The fundamental operation of the QRs are to distribute the entangled photon pairs between the two ends of the entire quantum channel, which is in principle sensitive to the lifetimes of their memories, is using multiplexed multimode quantum memories (MM-QMs) in each QR node [21].

To enable the building of quantum networks with improvements the entanglement distribution rate of QRs, multiplexing of quantum nodes is suggested to be implemented with MM-QMs and different types of multiplexed entangled photon sources. A multiplexing of quantum nodes are mainly insensitive to the coherence time of the quantum memory QM components as suggested by [22].

1.2 Aim of The Work

The aim of this work is to study entanglement distribution rate with short lifetime multiplexed multimode quantum memories, also to improve entanglement distribution rate of quantum repeater based on photon pair sources using different schemes, such as multiplexed photon pair source, single photon source and multiplexed single photon sources all with combination of multiplexed multimode quantum memory.

1.3 Fundamentals of Quantum Mechanics

Classical mechanics can explain macroscopic phenomena such as pendulum movement while, quantum mechanics is used to explain microscopic phenomena such as photon-atomic interference. Light behaves in some aspects like particles and in other aspects like waves. Particles and waves are distinguishable phenomena, with different properties and behaviour. In quantum mechanics, wave-particle duality is the concept that every quantum entity may be partly described in terms not only of particles, but also of waves. It expresses the inability of the classical concepts "particle or wave" to fully describe the behavior of quantum-scale objects [23].

Quantum mechanics shows that light along with all other forms of electromagnetic radiation, comes in discrete units called photons. A single

photon is a quantized shape of wave packet, or smallest observable amount of the electromagnetic field. So, quantum mechanics is a more accurate description of the microscopic world than classical mechanics and therefore, quantum information which is governed by the laws of quantum mechanics is a more accurate description of information theory. Quantum mechanics is the origin for accepting many quantum fields such as quantum computation and quantum communications. So, the main principles of quantum mechanics are [23]:

- 1- A system is completely described by a wave function, usually represented by ψ .
- 2- How ψ changes over time is given by the Schrödinger equation .
- 3- The description of nature is essentially probabilistic.
- 4- A probability amplitude is a complex number used in describing the behaviour of systems. Probability amplitudes provide a relationship between the wave function (or quantum state vector) of a system and the results of observations of that system.
- 5- It is not possible to know the values of all of the properties of the system at the same time. (Heisenberg's uncertainty principle)
- 6- Matter, like energy, exhibits a wave–particle duality.
- 7- Measuring devices are essentially classical devices, and measure classical properties such as position and momentum.

A wave function in quantum physics is a mathematical description of the quantum state of an isolated quantum system. The wave function is a complex-valued probability amplitude, and the probabilities for the possible results of measurements made on the system can be derived from it. According to the superposition principle of quantum mechanics, wave

functions can be added together and multiplied by complex numbers to form new wave functions and form a Hilbert space. The Hilbert space H can be defined as a real or complex inner product space. The Schrödinger equation, determines how wave functions evolve over time, because the Schrödinger equation is mathematically a type of wave equation. The state of any physical system in quantum mechanics, is entirely specified via a linear operator acting upon a complex Hilbert space [23].

1.3. 1 Dirac Notation and The Quantum State

For any system, the quantum state or state vector is described by unit vector in complex Hilbert space, which may also be recognized as state space, expressed by Hilbert space, which includes all possible pure quantum states of the given system. The quantum state is represented by ket vector $|v\rangle$, the basic item of linear algebra is the vector space. Table (1.1) reviews the Dirac notation of linear algebra. This *bra* $\langle \quad |$ *ket* notations are commonly utilized in quantum mechanic [24].

Table 1.1. Dirac notation [24].

Notation	Description
$ v\rangle$	"ket" Column vector.
$\langle v $	"bra" Row vector dual to $ v\rangle$.
$\langle\varphi v\rangle$	Inner product of vectors $\langle\varphi $ and $ v\rangle$.
$ \varphi\rangle\langle v $	Outer product of vectors $ \varphi\rangle$ and $\langle v $.
$ \varphi\rangle \otimes \langle v $	Tensor product of vectors $ \varphi\rangle$ and $\langle v $.
$ \varphi\rangle v\rangle$	Shortened notation for tensor product of $ \varphi\rangle$ and $ v\rangle$.
$ \varphi, v\rangle$	The abbreviated notation for tensor products of $ \varphi\rangle$ and $ v\rangle$.

A^*	Conjugate operator.
A^T	Transpose operator.
A^\dagger	Adjoint operator of A matrix. $A^\dagger = (A^T)^* = (A^*)^T$.
$\langle \varphi A \nu \rangle$	The inner product of $\langle \varphi $ and $A \nu \rangle$.

The inner product can be defined as a function which has two vectors as input $\langle \varphi |$ and $| \nu \rangle$ of a vector space which yields an output as a complex number. The tensor product $V \otimes W$ of two vector spaces V and W (over the same field) is itself a vector space. The tensor product of V and W is the vector space generated by the symbols $v \otimes w$, with $v \in V$ and $w \in W$, If we have a basis for the vector spaces, and the vector space is finite-dimensional, the vectors can be represented in terms of components under those basis vectors such as [25]:

$$v = \begin{bmatrix} v_1 \\ v_2 \\ \vdots \\ v_n \end{bmatrix}, \quad w = \begin{bmatrix} w_1 \\ w_2 \\ \vdots \\ w_m \end{bmatrix}$$

Given two vectors v and w , can form a tensor of their own from them rather naturally using the outer product, which is denoted $v \otimes w$ and equals vw^T , where T denotes the matrix transpose. This tensor comes out as the matrix:

$$|v\rangle \otimes \langle w| = \begin{bmatrix} v_1 w_1 & v_1 w_2 & \cdots & v_1 w_m \\ v_2 w_1 & v_2 w_2 & \cdots & v_2 w_m \\ \vdots & \vdots & \ddots & \vdots \\ v_n w_1 & v_n w_2 & \cdots & v_n w_m \end{bmatrix} \quad (1.1)$$

The tensor product structure is vital to consider the quantum mechanic of multipartite systems. In quantum computation, tensor product refers to the

degree of complexity of the quantum system, the two qbits system refers to the tensor product of two subsystems [25].

1.3.2 Linear Algebra and The Operators

Linear Algebra is essential for understanding quantum mechanics and the study of state space of a quantum system that is described as a vector spaces V which is inserted over the complex number field \mathbb{C} . Hilbert spaces have an orthogonal basis $B = \{\psi_1, \psi_2, \dots, \psi_n\}$. A wave function is a linear combination of the basis vectors. A basis of vector space V is a minimal collection of vectors $|v_1\rangle, \dots, |v_n\rangle$ such that every vector $|v\rangle \in V$. While the bases for n -dimension complex number (\mathbb{C}^n) can be represented as [26]:

$$\begin{bmatrix} 1 \\ 0 \\ \vdots \\ 0 \end{bmatrix}, \begin{bmatrix} 0 \\ 1 \\ \vdots \\ 0 \end{bmatrix}, \dots, \begin{bmatrix} 0 \\ 0 \\ \vdots \\ 1 \end{bmatrix} \text{ which can written as: } |0\rangle, \dots, |n-1\rangle.$$

Also, orthonormal bases can be described as vectors of unit length that are mutually orthogonal for instance $|0\rangle, |1\rangle$ and $\frac{1}{\sqrt{2}}(|0\rangle + |1\rangle), \frac{1}{\sqrt{2}}(|0\rangle - |1\rangle)$. However, the linear operator A is a function on any two vector spaces V and W , such that $A: V \rightarrow W$ as [26].

$$A(\alpha|w\rangle + \beta|v\rangle) = \alpha(A(|w\rangle)) + \beta(A(|v\rangle)) \quad (1.2)$$

Linear operators that act on wave functions can be represented as square matrices, if the vector space V has dimension n and vector space W has dimension m , then the operator A can be represented $n \times m$ matrix as [26]:

$$A = \begin{bmatrix} a_{0,0} & \cdots & a_{0,m-1} \\ \vdots & \ddots & \vdots \\ a_{n-1,0} & \cdots & a_{n-1,m-1} \end{bmatrix} \quad (1.3)$$

For example, the Pauli matrices that are helpful in investigation of quantum computation and also in quantum information. Pauli operators, as matrices are [26]:

$$\sigma_I = \begin{bmatrix} 1 & 0 \\ 0 & 1 \end{bmatrix} \textit{ do nothing} \quad (1.4)$$

$$\sigma_x = \begin{bmatrix} 0 & 1 \\ 1 & 0 \end{bmatrix} \textit{ bit flip} \quad (1.5)$$

$$\sigma_z = \begin{bmatrix} 1 & 0 \\ 0 & -1 \end{bmatrix} \textit{ bit flip} \quad (1.6)$$

$$\sigma_y = \begin{bmatrix} 0 & -i \\ i & 0 \end{bmatrix} \textit{ phase and phase flip} \quad (1.7)$$

In any system, an evolution operator changes a state vector to another state vector in the same state space. An effective physical evolution operator, must be unitary and Hermitian. Let A and B be the linear operators on a Hilbert space H , $|v\rangle \in H$, then [26]:

$$(AB)^\dagger = A^\dagger B^\dagger \quad (1.8)$$

$$(A|v\rangle)^\dagger = \langle v|A^\dagger \quad (1.9)$$

If linear operators are characterized on a vector space V this means that A is a linear operators from V to V , and can be described as [26]:

- 1- *Identity operator* I , if $A|v\rangle = |v\rangle$ for vectors $|v\rangle \in V$.
- 2- *Zero operator* O , if zero vector in the vector space denoted by 0 , which is used to satisfy any other vector $|v\rangle$ property, $|v\rangle + 0 = |v\rangle$.
- 3- *Hermitian* if $A^\dagger = A^{-1}$.
- 4- *Unitary* if $A^\dagger A = AA^\dagger = I$.

An eigenvector of a linear operator $A : V \rightarrow V$ is a non-zero vector such that $A|v\rangle = \lambda|v\rangle$, for some complex number λ where, λ is the eigenvalue corresponding to the eigenvector v , each operator has at least one

eigenvalue. A matrix (A) is diagonalizable if it can be written as $A = \sum_j \lambda_j |j\rangle\langle j|$, and $|j\rangle\langle j|$ is orthonormal basis [26].

1.3.3 The Density Operator

The quantum mechanic postulates could be written utilizing the density matrix. The density matrix is a representation of a linear operator called the density operator. Describing a quantum state by its density matrix is a fully other general formalism to describe a quantum state by its ket (state vector). However, in practice, it is often most suitable to use density matrices for calculations involving mixed states, and to use kets for calculations involving only pure states. The density operators formalism advantage is in describing different sub-systems of a multiple quantum system. In the density operator formalism, mixed quantum states are described ρ , such as [27]:

$$\rho = |v\rangle\langle v| \quad (1.10)$$

Where, $|v\rangle$ is the pure state. For a finite-dimensional function space, the most general density operator is of the form [27]:

$$\rho = \sum_{i=1}^n p_i |v_i\rangle\langle v_i| \quad (1.11)$$

Where the pure states $|v_i\rangle$ describe the system as a probabilistic combination of the probable states has classical probability distribution represented by p_i . The density operators involve all the possible information which can be taken out from the quantum system. In the density operator a quantum state represents a pure state which has the property $\rho^2 = \rho$, while for mixed states $\rho^2 \neq \rho$, More generally, mixed states commonly arise from a statistical mixture of the starting state from uncertainty in the preparation

procedure, such as slightly different paths that a photon can travel, or from looking at a subsystems entangled with each other.

The density operator satisfies the conditions [27]:

1- Normalization: The trace (tr) of A matrix is defined as:

$$tr(A) = a_{11} + a_{22} + \dots + a_{nn} = \sum_i a_{ii} \quad (1.12)$$

Where: a_{ii} are the elements of the main diagonal.

2- $tr(\rho) = 1 \Rightarrow \sum_i p_i = 1$ (sum of eigenvalues is 1).

3- Positivity: $p_i > 0$ (non-negative eigenvalues).

4- Hermiticity: $\rho^\dagger = \rho, \rightarrow p_i = p_i^*$ (Real eigenvalues).

To represent significant properties of the density operator, the trace operation can be used. In linear algebra, the trace of density operators an ($n - by - n$) square matrix A , is defined to be the sum of the elements on the main diagonal of A . The quantum state can be characterized using a density operator ρ which is a pure state if $tr(\rho^2) = 1$. Otherwise ($tr(\rho^2) < 1$), the state is a mixed state. Assume (A and B) be linear operators and $\eta = \mathbb{C}$, then [27]:

- $tr(AB) = tr(BA)$. (cyclic property)
- $tr(A + B) = tr(A) + tr(B)$ (linear property)
- $tr(\eta A) = \eta tr(A)$
- Trace is not modified under the unitary transformation:

$$A \rightarrow UAU^\dagger: \quad tr(UAU^\dagger) = tr(UU^\dagger A) = tr(A) \quad (1.13)$$

The measurement of A be an observable of the system, and suppose the ensemble is in a mixed state such that each of the pure states $|v_i\rangle$ occurs with probability p_i . The expectation value of the measurement can be calculated by extending from the case of pure states [27] :

$$\begin{aligned} \langle A \rangle &= \sum_i p_i \langle v_i | A | v_i \rangle = \sum_i p_i tr(|v_i\rangle \langle v_i | A) = \sum_i tr(p_i (|v_i\rangle \langle v_i | A) = \\ &tr(\sum_i p_i (|v_i\rangle \langle v_i | A) = tr(\rho A) \end{aligned} \quad (1.14)$$

Thus, the familiar expression $\langle A \rangle = \langle \nu | A | \nu \rangle$, for pure states is replaced by [27]:

$$\langle A \rangle = \text{tr}(\rho A) \quad (1.15)$$

For mixed states: if A has spectral resolution [27]:

$$A = \sum_i a_i |a_i\rangle\langle a_i| = \sum_i a_i p_i \quad (1.16)$$

Where, $P_i = |a_i\rangle\langle a_i|$, the corresponding density operator after the measurement is given by [27]:

$$\rho' = \sum_i p_i \rho p_i \quad (1.17)$$

The above density operator describes the full ensemble after measurement. The sub-ensemble for which the measurement result was the specific value a_i is described by the different density operator [27]:

$$\rho'_i = \frac{P_i \rho P_i}{\text{tr}[\rho P_i]} \quad (1.18)$$

The density matrices are a basic tool of quantum mechanics, and quantum computation calculation. Some specific examples where density matrices are especially helpful and common are as follows [27]:

- Quantum decoherence theory typically involves non-isolated quantum systems developing entanglement with other systems, including measurement apparatuses. Density matrices make it much easier to describe the process and calculate its consequences.
- Similarly, in quantum computation, quantum information theory, and other fields where state preparation is noisy and decoherence can occur, density matrices are frequently used.
- Quantum tomography is the process of experimentally measuring the density matrix of a system.

A density operator ρ_{AB} can be describing the composed states of physical systems A and B . The reduced density operator ρ_A for system A can be defined as [27]:

$$\rho_A = \text{tr}_B(\rho_{AB}) \quad (1.19)$$

Where tr_B , is the trace matrix of system B.

1.3.4 The Postulates of Quantum Mechanics

Quantum mechanics is mathematical representation and interpretation of any physical theories. It doesn't tell us what rules this system obey. The four postulates of quantum mechanics give an association between the mathematical formalism of quantum mechanics and the physical system. The postulates of quantum mechanics determined after long procedure of trials and errors, that included lot of searching and guessing by the originators of the theory. The quantum mechanic postulates with the support of density operators can be summarized as follows [27]:

Postulate 1: The state space, related to any physical system which is a complex vector space with inner product (*Hilbert space* H) known as the state space of the system. The state vector is entirely describing the state of its system, which is a unit vector in the system's state space as:

$$|\psi\rangle = \alpha_0|0\rangle + \alpha_1|1\rangle \quad (1.20)$$

Postulate 2: The evolution of any closed quantum system described by the unitary transformation. In which states $|\psi\rangle$ and $|\psi'\rangle$ in times t_1 and t_2 respectively are connected by the unitary operator U , which is related to these times only:

$$|\psi'\rangle = U|\psi\rangle \quad (1.21)$$

Schrodinger equation describes the time evolution of the quantum system state:

$$i\hbar \frac{\partial}{\partial t} |v\rangle = \mathcal{H} |v\rangle \quad (1.22)$$

Where: \hbar is the reduced Planck constant, $\hbar \approx 1.055 \times 10^{-34}$ Js. And \mathcal{H} is a stable Hermitian operator called the Hamiltonian of the system. Actually, it is an appropriate to absorb \hbar into \mathcal{H} , effectually setting $\hbar = 1$. The Schrodinger equation solution's (1.20) establishes an operator of time evolution is [27]:

$$U(\Delta t) = e^{-iH\Delta t} \quad (1.23)$$

The operator of time evolution is $U(\Delta t)$, it is a unitary operator since the Hamiltonian \mathcal{H} is a Hermitian matrix, $\mathcal{H} = \mathcal{H}^\dagger$, thus the unitarity condition is satisfied as [27]:

$$U(\Delta t)U(\Delta t)^\dagger = e^{-iH\Delta t} e^{iH\Delta t} = I \quad (1.24)$$

The second postulate can reformulate utilizing unitary evolution as:

The closed quantum system time evolution of the state $|v_1\rangle$ at time (t_1) to the state $|v_2\rangle$ at time (t_2) is defined using a unitary operator $U = U(t_2 - t_1)$ [27]:

$$|v_2\rangle = U |v_1\rangle \quad (1.25)$$

Postulate 3: Quantum measurement, $\{M_m\}$ represents the assembly of the quantum measurement operators. The measurement operators can be performed on the state space of the system demanded to be measured.. The system state $|v\rangle$ measured may give as [27]:

$$P(r_m) = \langle v | M_m^\dagger M_m | v \rangle \quad (1.26)$$

The system state $|v\rangle$ outcome is r_m with probability $P(r_m)$. the index m denotes to the measurement result r_m which may arise in the experiment. So, the state of the system after measurement is [27]:

$$|v'\rangle = \frac{M_m|v\rangle}{\sqrt{P(r_m)}} \quad (1.27)$$

The operators $\{M_m\}$ satisfy the completeness equation:

$$\sum_m M_m^\dagger M_m = I \quad (1.28)$$

Utilizing the completeness equation (1.28) composed with the normalization condition, their probabilities sum is one [27]:

$$\sum_m P(r_m) = \sum_m \langle v|M_m^\dagger M_m|v\rangle = 1 \quad (1.29)$$

A projective measurement P_m tolerates to state the measurement, in an orthonormal basis $|m\rangle$ principally as [27]:

$$P_m = |m\rangle\langle m| \quad (1.30)$$

Postulate 4: Composite systems: tensor product of the subsystems states spaces represents the composite system state. If the state space S of the tensor product of the state spaces S_i of composite physical system, then its constituents are [27]:

$$S = \otimes_i S_i \quad (1.31)$$

Additionally, if the sub-systems are in the states $|v_i\rangle \in S_i$, later the joint state $|v\rangle \in S$ of the entire system is [27]:

$$|v\rangle = \otimes_i v_i \quad (1.32)$$

1.4 Quantum Computing

Quantum computing relies on the quantum phenomena, such as the quantum entanglement and superposition to execute the calculations and

manipulate data. The classical computing requires the data that can be encoded into binary digits (classical bits 0 or 1), while qubit is used in quantum computation, that can be in a superposition state. The quantum computing can operate the qubit using quantum gates [28].

1.4.1 Quantum Bit (Qubit)

In quantum computing, a qubit or quantum bit is the basic unit of quantum information and the quantum version of the classical binary bit physically realized with a two-state device. A qubit is a two-state level quantum system. The qubit, physically can be represented by the time bin encoding , the polarization of a single photon in which the two states can be taken to be the vertical polarization and the horizontal polarization or the spin of the electron in which the two levels can be taken as spin up and spin down. In a classical system, a bit would have to be in one state or the other such as (0 or 1) [28].

However, quantum mechanics allows the qubit to be in a coherent superposition of both states/levels simultaneously, a property which is fundamental to quantum mechanics and quantum computing. The basic data unit in a classical communication is the bit (0 or 1). while in quantum computation, a quantum bit is used that can be in a superposition state, which is shortened to qubit (0 and 1). Superposition states allow many computations to be performed simultaneously, and gives rise to what is known as quantum parallelism. Quantum parallelism is an important property of quantum computing. It is based on using the calculations that are superpositions of the base states that can simultaneously produce a large number of calculations with various input data. A quantum superposition state allows a qubit to store (0 and 1) simultaneously. Two qubits can store all the 4 binary numbers 00, 01, 10 and 11 simultaneously. Three qubits

stores the 8 binary numbers 000, 001, 010, 011, 100, 101, 110 and 111 simultaneously and so on as binary numbers = 2^N , where N = qubit number [28].

So, what is the qubit?

- The quantum bit (qubit) is the smallest quantum information unit.
- Qubits are often made of subatomic particles such as:
 - ✓ Photons
 - ✓ Coherent state of light
 - ✓ Electrons
 - ✓ Quantum dot
 - ✓ Optical lattice

The problems related with the qubit:

- Observer effect
 - ✓ Qubit cannot be observed without destroying their state.
- Decoherence
 - ✓ Decoherence occurs when a system interacts with its environment.

A single qubit can be described by a vector two dimensional complex Hilbert space. Also, qubits can be represented by an arbitrary superposition of two-state system as:

$$|\psi\rangle = \alpha|0\rangle + \beta|1\rangle \quad (1.33)$$

Where, $|1\rangle$ and $|0\rangle$ represent any orthonormal basis in the state space, and α, β are complex numbers, called amplitudes, associated with the basis states, the qubit state vector must have unit norm, $|\alpha|^2 + |\beta|^2 = 1$. In quantum mechanics, the Bloch sphere as shown in Fig. (1.1), is a geometrical

representation of the qubit. Given an orthonormal basis, any pure state $|\psi\rangle$ of a two-level quantum system can be written as a superposition of the basis vectors $|1\rangle$ and $|0\rangle$. From quantum mechanics that the total probability of the system has to be one: $\langle\psi|\psi\rangle = 1$, where $|\psi\rangle$ can rewrite the qbit as [28]:

$$|\psi\rangle = \cos\left(\frac{\theta}{2}\right)|0\rangle + e^{i\varphi}\sin\left(\frac{\theta}{2}\right)|1\rangle \quad (1.34)$$

Where: $(0 \leq \theta \leq \pi)$ and $(0 \leq \varphi \leq 2\pi)$.

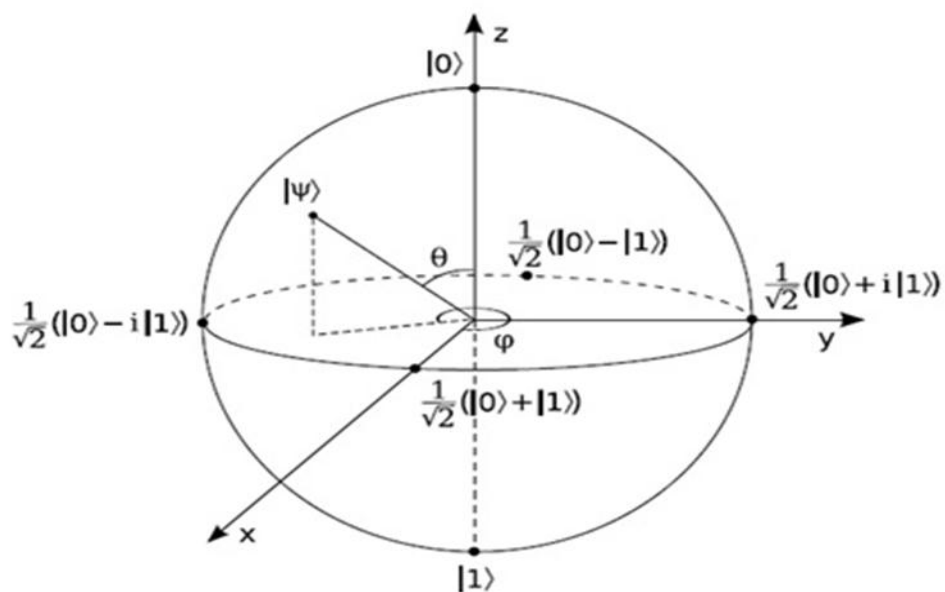


Fig. 1.1: The representation of qubit on Bloch sphere. The state of the qubit can be defined by the angles that create a unit vector that points from the origin to the surface of the sphere $|\psi\rangle = \alpha|0\rangle + \beta|1\rangle = \cos\left(\frac{\theta}{2}\right)|0\rangle + e^{i\varphi}\sin\left(\frac{\theta}{2}\right)|1\rangle$. θ determines the relative amplitudes of the two basis states while φ defines the phase between the two components of the vector [28].

The qubit, physically can be represented by, time bin encoding that is a technique used in quantum information science to encode a qubit of information on a photon, spin directions of an electrons in the magnetic field, or individual polarization states of a photon. The related state space of two dimensional complex Hilbert space H_2 , that is crossed by an orthonormal

basis $\mathcal{B} = \{|1\rangle, |0\rangle\}$. The $|1\rangle$ and $|0\rangle$ raises to the typical (computational) basis well-defined as [28]:

$$|0\rangle = \begin{pmatrix} 1 \\ 0 \end{pmatrix} \text{ and } |1\rangle = \begin{pmatrix} 0 \\ 1 \end{pmatrix} \longrightarrow \text{(Standard basis)}$$

The tensor product of the individual sub-system states represent the combined state of a composed system. If the two qubits $|v\rangle, |\varphi\rangle \in H_2$, $|v\rangle = \alpha|0\rangle + \beta|1\rangle$, $|\varphi\rangle = \gamma|0\rangle + \delta|1\rangle$. Their tensor product is equal to [28]:

$$|v\rangle|\varphi\rangle = \alpha\gamma|0\rangle|0\rangle + \alpha\delta|0\rangle|1\rangle + \beta\gamma|1\rangle|0\rangle + \beta\delta|1\rangle|1\rangle \quad (1.35)$$

This equation can be written as [28]:

$$|v\rangle|\varphi\rangle = \alpha_{00}|00\rangle + \alpha_{01}|01\rangle + \alpha_{10}|10\rangle + \alpha_{11}|11\rangle = \sum_{i \in \{0,1\}^2} \alpha_i |i\rangle \quad (1.36)$$

States: $|00\rangle$, $|01\rangle$, $|10\rangle$ and $|11\rangle$ are the typical basis vectors of Hilbert space H as [28]:

$$\begin{aligned} |00\rangle &= \begin{pmatrix} 1 \\ 0 \end{pmatrix} \otimes \begin{pmatrix} 1 \\ 0 \end{pmatrix} = \begin{pmatrix} 1 \\ 0 \\ 0 \\ 0 \end{pmatrix}, & |01\rangle &= \begin{pmatrix} 1 \\ 0 \end{pmatrix} \otimes \begin{pmatrix} 0 \\ 1 \end{pmatrix} = \begin{pmatrix} 0 \\ 1 \\ 0 \\ 0 \end{pmatrix} \\ |10\rangle &= \begin{pmatrix} 0 \\ 1 \end{pmatrix} \otimes \begin{pmatrix} 1 \\ 0 \end{pmatrix} = \begin{pmatrix} 0 \\ 0 \\ 1 \\ 0 \end{pmatrix}, & |11\rangle &= \begin{pmatrix} 0 \\ 1 \end{pmatrix} \otimes \begin{pmatrix} 0 \\ 1 \end{pmatrix} = \begin{pmatrix} 0 \\ 0 \\ 0 \\ 1 \end{pmatrix} \end{aligned}$$

The (00, 01, 10, 11) can be named again to (0, 1, 2, 3) since they can be simply seen as a binary symbol of these integers [28].

An example of a qubit as a photon (a particle of light) travelling along two possible paths. Consider what happens when a photon encounters a beam splitter as shown in Figure (1.2). A beam splitter is just like an ordinary mirror, however the reflective coating is made so thin that not all light is reflected and some light is transmitted through the mirror as well. When a

single photon encounters a beam splitter, the photon emerges in a superposition of the reflected path and the transmitted path. One path is taken to be the binary number 0, and the other path is taken to be the number 1. The photon is in a superposition of both paths and so represents both 0 and 1 simultaneously [29].

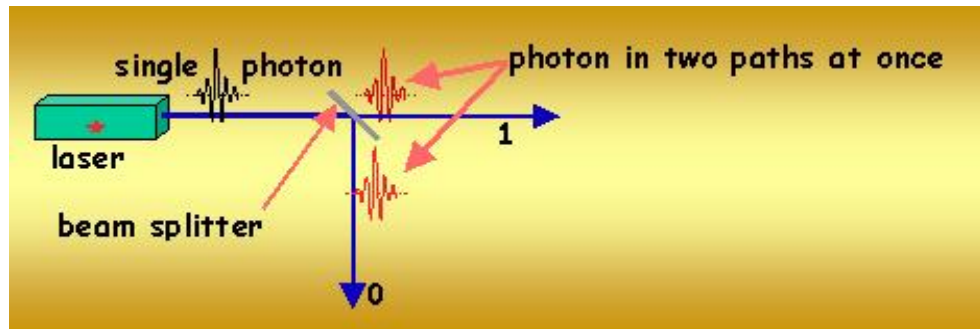


Fig. 1.2: A qubit as a photon (a particle of light) travelling along two possible paths when a photon encounters a beam splitter [29].

However, photons which can be provided from laser source are ideal carriers for quantum information processing and quantum communication since they are easy to be generated and manipulated. But, the most important problem is that photons suffer from that they can not be stored and experience losses during the transmission [30].

1.4.2 Quantum Entanglement

Quantum entanglement is a physical phenomenon which arises when pairs of particles are generated or shared spatial closeness in ways such that the quantum state of each particle cannot be described independently of the state of the other, even when the particles are separated by a large distance. Composite quantum systems obviously decompose into two or more sub-systems, where every sub-system itself is a suitable quantum system.

Further, product states that represent a composite system involves many independent states combined by means of tensor product, correspondingly to classical composite systems, quantum mechanics proposals an exclusive new phenomenon known entanglement. For instance, entangled states can be represented by the four *Bell states* [31]:

$$|\Phi^+\rangle = \frac{1}{\sqrt{2}}(|00\rangle + |11\rangle) \quad (1.37)$$

$$|\Phi^-\rangle = \frac{1}{\sqrt{2}}(|00\rangle - |11\rangle) \quad (1.38)$$

$$|\Psi^+\rangle = \frac{1}{\sqrt{2}}(|01\rangle + |10\rangle) \quad (1.39)$$

$$|\Psi^-\rangle = \frac{1}{\sqrt{2}}(|01\rangle - |10\rangle) \quad (1.40)$$

These four Bell state vectors of the state space of two qubits form an orthonormal basis. The *measurement on this basis is called a Bell state measurement (BSM)* [32].

1.5 The Quantum Gates

Quantum gates are used to implement many processes on the qubit of quantum computing. However, a common set of quantum gates means it involve a finite set of processes that can be concatenated to implement any individual operation. Dirac notation of the quantum gates is $\sum_i |input_i\rangle\langle output_i|$, quantum gates have two types which are [33]:

1.5.1 Single-input gates

One-input gate is called single-qubit gates, for example:

1- Hadamard gate

The Hadamard gate acts on a single qubit. The hadamard gate is a one input gate. It maps input $|0\rangle$ to $\frac{|0\rangle+|1\rangle}{\sqrt{2}}$, and input $|1\rangle$ to $\frac{|0\rangle-|1\rangle}{\sqrt{2}}$. which means that a measurement will have equal probabilities to become 1 or 0 (i.e. creates a superposition). A Hadamard gate has a matrix form as [33]:

$$\begin{aligned} Had &= |0\rangle \left[\frac{\langle 0| + \langle 1|}{\sqrt{2}} \right] + |1\rangle \left[\frac{\langle 0| - \langle 1|}{\sqrt{2}} \right] \\ &= \frac{1}{\sqrt{2}} [|0\rangle\langle 0| + |0\rangle\langle 1| + |1\rangle\langle 0| - |1\rangle\langle 1|] \\ Had &= \frac{1}{\sqrt{2}} \begin{bmatrix} 1 & 1 \\ 1 & -1 \end{bmatrix} \end{aligned} \quad (1.41)$$

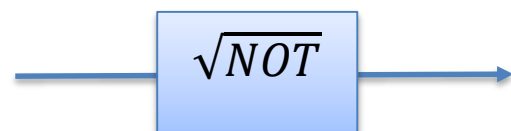


2- Square root of NOT gate (\sqrt{NOT}):

The square root of NOT gate acts on a single qubit. It maps the basis state $|0\rangle$ to $\frac{(1+i)|0\rangle+(1-i)|1\rangle}{2}$ and $|1\rangle$ to $\frac{(1-i)|0\rangle+(1+i)|1\rangle}{2}$, some matrix elements are imaginary as [33]:

$$\sqrt{NOT} = \frac{1}{\sqrt{2}} \begin{bmatrix} i & 1 \\ 1 & i \end{bmatrix} \quad (1.42)$$

$\therefore \sqrt{NOT} \times \sqrt{NOT} = NOT$ gate



3- Phase shift gate:

This is a single-qubit gates that leave the basis state $|0\rangle$ unchanged and map $|1\rangle$ to $e^{i\phi}|1\rangle$. The probability of measuring a $|0\rangle$ or $|1\rangle$ is unchanged

after applying this gate, however it modifies the phase of the quantum state. Phase shift gate R is one input gate with a matrix form as [33]:

$$R_{\phi} = \begin{bmatrix} 1 & 0 \\ 0 & e^{i\phi} \end{bmatrix} \quad (1.43)$$



1.5.2 Two-input gates:

Two-input gate called two- qubit gates, for example are:

1- Controlled NOT Gate (CNOT)

CNOT gate has two inputs qubit identified, such control qubit and target qubit singly. The CNOT representation is shown in the Figure (1.3), the upper line describes the *control qubit*, while the lower line describes the *target qubit*. The gate action may be defined in this way [33]:

- ❖ If the *control qubit* is set to (0), then the *target qubit* is left unchanged.
- ❖ If the *control qubit* is set to (1), then the *target qubit* is flipped.

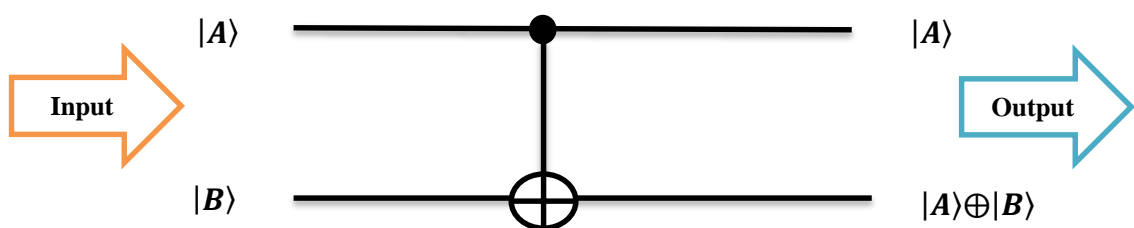


Fig. 1.3 of CNOT gate [33].

The truth table 1.2 of CNOT gate is:

Truth table 1.2 of CNOT gate

Input	Output
$ 00\rangle$	$ 00\rangle$
$ 01\rangle$	$ 01\rangle$
$ 10\rangle$	$ 11\rangle$
$ 11\rangle$	$ 10\rangle$

To illustrate the operation of the CNOT gate which is shown in Figure (1.3), let \hat{U}_{CNOT} as [33]:

$$\hat{U}_{CNOT}|00\rangle = |00\rangle$$

$$\hat{U}_{CNOT}|01\rangle = |01\rangle$$

$$\hat{U}_{CNOT}|10\rangle = |11\rangle$$

$$\hat{U}_{CNOT}|11\rangle = |10\rangle$$

That is briefly expressed if the controlled *qubit* is $|1\rangle$, flip the second. The process of realizing this *two – qubit* quantum gate is closely linked to the idea of entanglement as [33]:

$$\begin{aligned}
|\psi\rangle_{un}\hat{U}_{CNOT} &= \left(\frac{1}{\sqrt{2}}(|0\rangle_a|0\rangle_b + |1\rangle_a|0\rangle_b)\right)\hat{U}_{CNOT} \\
&= \frac{1}{\sqrt{2}}(\hat{U}_{CNOT}|0\rangle_a|0\rangle_b + \hat{U}_{CNOT}|1\rangle_a|0\rangle_b) \\
&= \frac{1}{\sqrt{2}}(|0\rangle_a|0\rangle_b + |1\rangle_a|1\rangle_b) \tag{1.44}
\end{aligned}$$

So, the CNOT gate converts the un-entangled state $|\psi\rangle_{un}$ into the entangled state $|\psi\rangle_{en}$, in few words CNOT gate is entangling gate.

From Dirac notation of CNOT gate derived from its truth table 1.2, the matrix of CNOT gate is [33]:

$$\text{CNOT} = \sum_i |input_i\rangle\langle output_i| \quad (1.45)$$

CNOT gate inputs and output matrices are:

$$|00\rangle = |0\rangle \otimes |0\rangle = \begin{bmatrix} 1 \\ 0 \\ 0 \\ 0 \end{bmatrix}, \quad |01\rangle = |0\rangle \otimes |1\rangle = \begin{bmatrix} 0 \\ 1 \\ 0 \\ 0 \end{bmatrix}$$

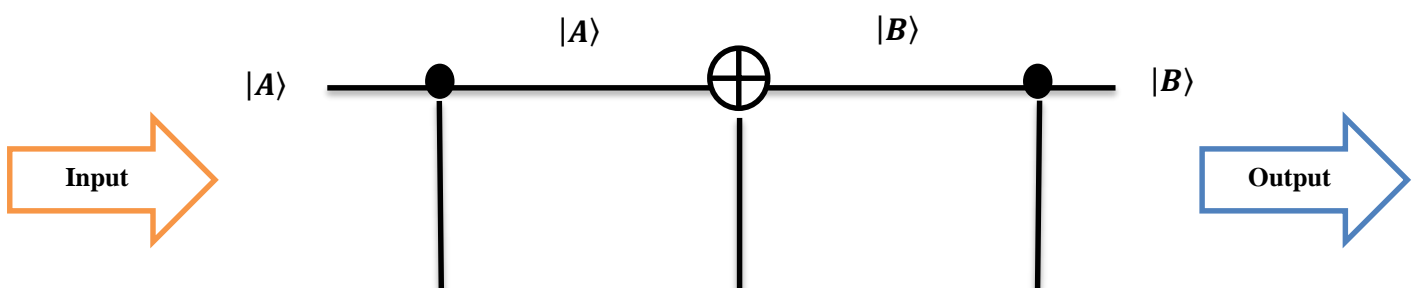
$$|10\rangle = |1\rangle \otimes |0\rangle = \begin{bmatrix} 0 \\ 0 \\ 1 \\ 0 \end{bmatrix}, \quad |11\rangle = |1\rangle \otimes |1\rangle = \begin{bmatrix} 0 \\ 0 \\ 0 \\ 1 \end{bmatrix}$$

$$\therefore \text{CNOT} = |00\rangle\langle 00| + |01\rangle\langle 01| + |10\rangle\langle 11| + |11\rangle\langle 10|$$

$$\begin{aligned} &= \begin{bmatrix} 1 \\ 0 \\ 0 \\ 0 \end{bmatrix} [1 \ 0 \ 0 \ 0] + \begin{bmatrix} 0 \\ 1 \\ 0 \\ 0 \end{bmatrix} [0 \ 1 \ 0 \ 0] + \begin{bmatrix} 0 \\ 0 \\ 1 \\ 0 \end{bmatrix} [0 \ 0 \ 0 \ 1] \\ &\quad + \begin{bmatrix} 0 \\ 0 \\ 0 \\ 1 \end{bmatrix} [0 \ 0 \ 1 \ 0] \\ &= \begin{bmatrix} 1 & 0 & 0 & 0 \\ 0 & 1 & 0 & 0 \\ 0 & 0 & 0 & 1 \\ 0 & 0 & 1 & 0 \end{bmatrix} \end{aligned} \quad (1.46)$$

2- SWAP Gate

Using three CNOT gates as shown in Figure (1.4), swap gate could be prepared and it can be used for entanglement swapping operation. It swaps the states of the two-qubits, see table 1.3 [33].



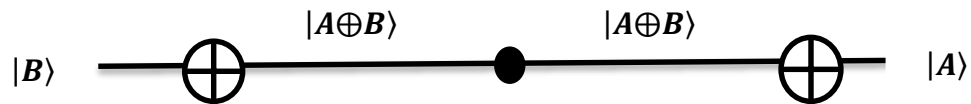


Fig. 1.4 of Swap gate [33].

While the truth table of swap gate is:

Truth Table 1.3 of Swap gate

Input	Output
$ 00\rangle$	$ 00\rangle$
$ 01\rangle$	$ 10\rangle$
$ 10\rangle$	$ 01\rangle$
$ 11\rangle$	$ 11\rangle$

The implementation sequence of swap gate is as follows:

- 1- The inputs are $|A, B\rangle$. The output of first CNOT gate is $|A, A\oplus B\rangle$.
- 2- This $|A, A\oplus B\rangle$ is served to the second CNOT gate and out of the second CNOT gate is $|A\oplus(A\oplus B), A\oplus B\rangle = |B, A\oplus B\rangle$.
- 3- The output of third CNOT gate is $|B, B\oplus(A\oplus B)\rangle = |B, A\rangle$.

From Dirac notation of SWAP gate derived from its truth table 1.3, the matrix of SWP gate is [33]:

$$\begin{aligned}
 \text{SWAP} &= \sum_i |input_i\rangle\langle output_i| \\
 &= |00\rangle\langle 00| + |01\rangle\langle 10| + |10\rangle\langle 01| + |11\rangle\langle 11|
 \end{aligned}$$

$$\begin{aligned}
&= \begin{bmatrix} 1 \\ 0 \\ 0 \\ 0 \end{bmatrix} [1 \ 0 \ 0 \ 0] + \begin{bmatrix} 0 \\ 1 \\ 0 \\ 0 \end{bmatrix} [0 \ 0 \ 1 \ 0] + \begin{bmatrix} 0 \\ 0 \\ 1 \\ 0 \end{bmatrix} [0 \ 1 \ 0 \ 0] \\
&\quad + \begin{bmatrix} 0 \\ 0 \\ 0 \\ 1 \end{bmatrix} [0 \ 0 \ 0 \ 0] \\
&= \begin{bmatrix} 1 & 0 & 0 & 0 \\ 0 & 0 & 1 & 0 \\ 0 & 1 & 0 & 0 \\ 0 & 0 & 0 & 1 \end{bmatrix} \tag{1.47}
\end{aligned}$$

1.6 Quantum Communication

Quantum communication is a field aims to exploit the quantum mechanics phenomena such as entanglement that has no counterpart in classical system. Also, quantum communication provides a means for secure communication in open channels and higher channel capacity. One of the primary goals of quantum communication is to develop the ability to communicate to arbitrary distances. Communication distances limited to a few hundred kilometers due to photon loss. So, the QR was suggested to extend the quantum communication distance. The QR implementation requirements are the long distance quantum communication protocols and the ingredients of QR. Entangled light particles, photons, are the fundamental resource used in quantum communication to distribute a secure encryption key. The field of quantum communications agrees with the distribution of quantum information typically carried by photons provided by laser source, over long distances. However, long distance quantum communications are done by many protocols such as quantum teleportation and entanglement swapping, which mainly depend on the establishment of entangled photon between the entire points of the channel [34].

Quantum teleportation, is a technique for transmitting an arbitrary quantum state from one position to another without any physical movement containing the state through the superseding space. This can be achieved with the assistance of a supplementary bipartite entangled state, one subsystem of which is near the state to be teleported, the other subsystem will hold the quantum state after the teleportation is complete, Figure (1.5) [5].

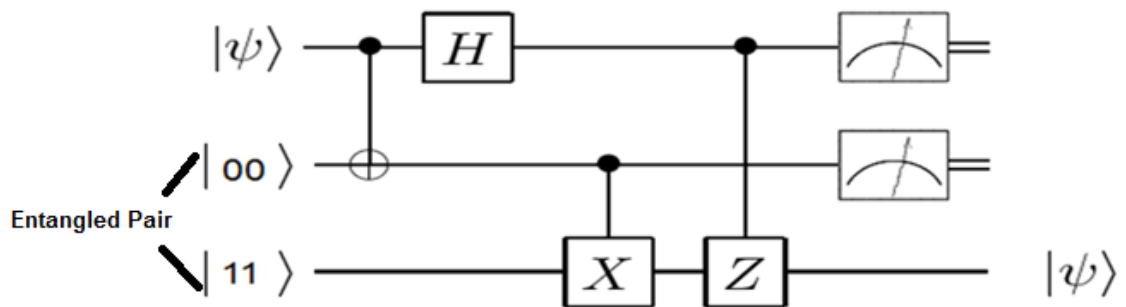


Fig. 1.5: Quantum teleportation scheme. A quantum state $|\psi\rangle$ transmitted from one location to another with assistance of CNOT gate, Hadamard gate H, entangled pair and Pauli transformation X and Z [35].

For instance: If "Alice and Bob" share an entangled state, and Alice (Bob) can transmit an unknown quantum state to Bob (Alice) without physically moving the unknown state through a process called quantum teleportation [4]. Suppose Alice holds the qubit state $|\Psi\rangle_C = \alpha|0\rangle + \beta|1\rangle$, she and Bob share any Bell state $|\Psi\rangle_{AB}$ (Choosing the Bell state $|\Phi^+\rangle$ state for this example). The entire composite system is then termed by [36]:

$$|\Psi\rangle_{AB} |\Psi\rangle_C = |\Phi^+\rangle_{AB} (\alpha|0\rangle + \beta|1\rangle) \quad (1.48)$$

$$\begin{aligned} |\Psi\rangle_{ABC} &= \frac{1}{\sqrt{2}} (|00\rangle + |11\rangle) (\alpha|0\rangle + \beta|1\rangle) \\ &= \frac{1}{\sqrt{2}} (\alpha|000\rangle + \alpha|110\rangle + \beta|001\rangle + \beta|111\rangle) \end{aligned} \quad (1.49)$$

If Alice performs a BSM on the two *qubits* in her possession, then conditional on Alice's measurement result Bob efficiently gets one of the following states [36]:

$$\langle \Phi_{AC}^+ | \varphi_{ABC} \rangle \rightarrow \alpha |0\rangle_B + \beta |1\rangle_B \quad (1.50)$$

$$\langle \Phi_{AC}^- | \varphi_{ABC} \rangle \rightarrow \alpha |0\rangle_B - \beta |1\rangle_B \quad (1.51)$$

$$\langle \Psi_{AC}^+ | \varphi_{ABC} \rangle \rightarrow \beta |0\rangle_B + \alpha |1\rangle_B \quad (1.52)$$

$$\langle \Psi_{AC}^- | \varphi_{ABC} \rangle \rightarrow \beta |0\rangle_B - \alpha |1\rangle_B \quad (1.53)$$

Where each state occurs with a probability of (1/4). Depending on the measurement outcome of the BSM from Alice, Bob can apply a phase flip and/or a bit flip to correct his state, as characterized in (table 1.4) Bob then holds a state that is identical to $|\Psi\rangle_C$ original held by Alice. So as to perform the teleportation, they proceed as follows [36]:

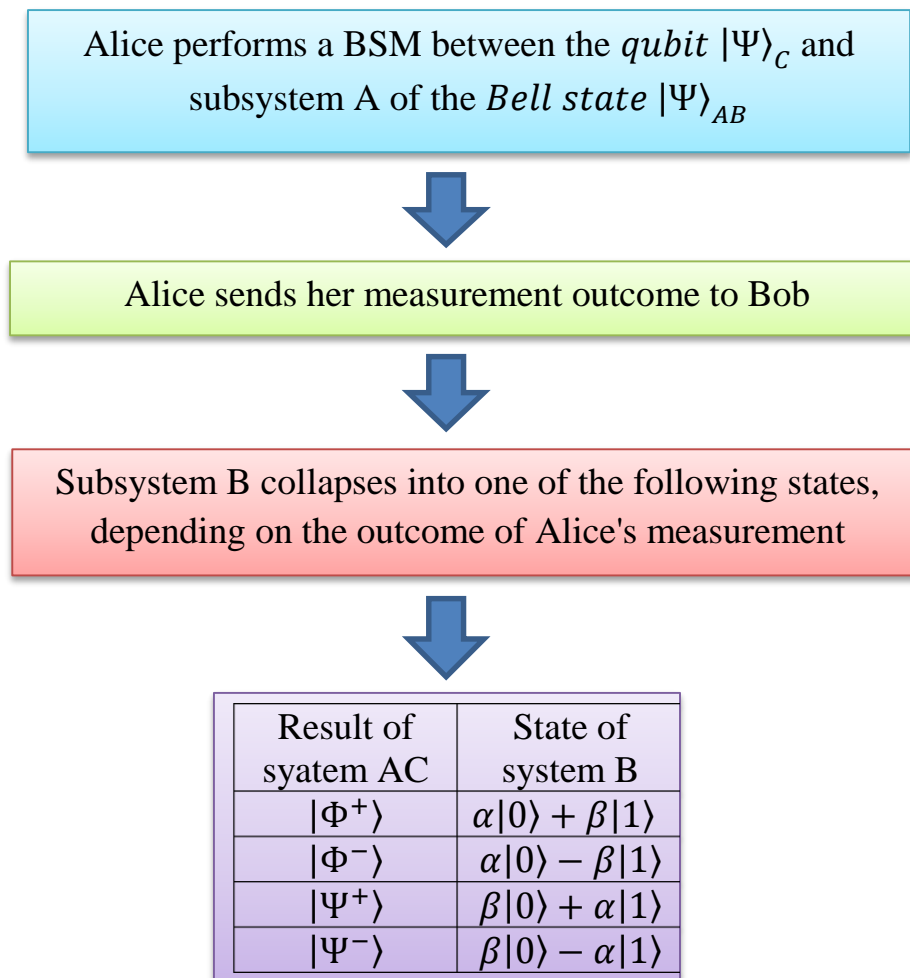


Fig. 1.6: Quantum teleportation performing steps.

Depending on what Alice sends him, Bob sends system B through a unitary channel described by one of the following operators illustrated in table 1.4 as:

Table 1.4. Bob's correctional Pauli operation on his *qubit*, depending on the Bell state measurement outcome [36].

Bell state measurement outcome (Result)	Unitary	Bob's operation
$ \Phi^+\rangle$	I	Do nothing
$ \Phi^-\rangle$	Z	Phase flip
$ \Psi^+\rangle$	X	Bit flip
$ \Psi^-\rangle$	ZX	Bit and phase flip

Here, X and Z are Pauli matrices. After this correction, system B ends up in the state $|\Psi\rangle_B = \alpha|0\rangle + \beta|1\rangle$. Several properties of quantum teleportation are to be noted as [36]:

1. Alice does not need to know what $|\Psi\rangle_A$ is. In order to teleport it, all that is necessary is that she measure it jointly with one subsystem of a Bell state.
2. after the teleportation is finished. Alice only has a random Bell state; she no longer has a copy of $|\Psi\rangle_A$.
3. Bob cannot construct $|\Psi\rangle_B$ without receiving Alice's measurement result. Conversely, the information sent from Alice to Bob is, by itself, not sufficient to reconstruct the state $|\Psi\rangle_A$.

Entanglement swapping uses the same principle as quantum teleportation. Assume there is an intermediate party, called Charlie, between Alice and Bob. If (Alice and Charlie) and (Bob and Charlie), each share an entangled state, for example a maximally entangled Bell state $|\Phi^+\rangle$, then Charlie can perform a *Bell state measurement BSM* on his two qubit states, resulting in (Alice and Bob) sharing an entangled bipartite

state. Later, Charlie can implement a BSM, he communicates his measurement outcome to Bob (or Alice). Bob (or Alice) can then correct their state with the same operations as the quantum teleportation scheme used in table 1.4. This is a key principle used for many quantum repeater schemes, allowing for generation of entanglement between two spatially separated parties as shown in Figure (1.7) [37].

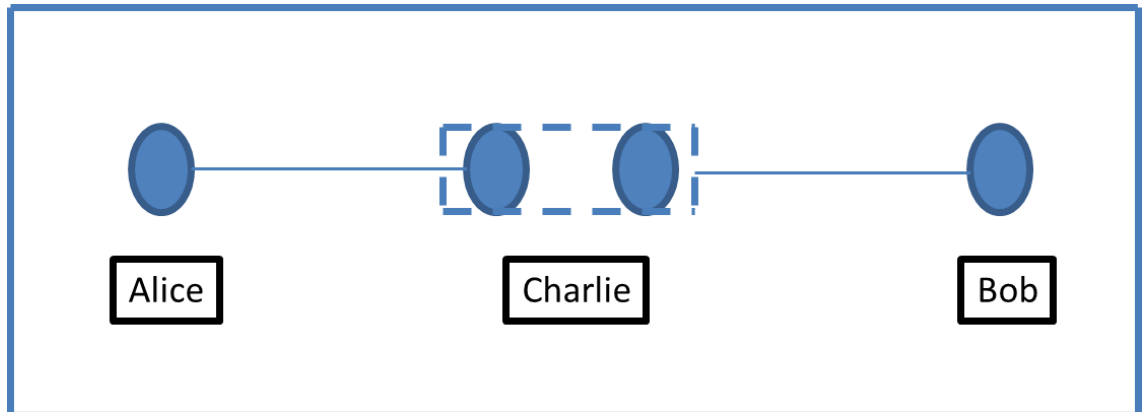


Fig. 1.7: A quantum repeater scheme. Dots represent quantum memories, lines show entanglement, and dashed boxes indicate Bell state measurements.

While the ingredients of QR are:

- 1- The quantum memory.
- 2- BSM.
- 3- Entangled photon source.

By reason of photon losses and no-cloning theorem, strong quantum communications via long lossy channels needs quantum repeaters to achieve the ultimate goal of long-distance quantum communication. These imperfections also limit the entanglement distribution rate, which will affect the efficiency of the system. A QR, can allow for communication with rate higher than what is achievable over direct transmission through a loss only channel. The QRs with effective single-photon source and quantum memories presented here to improve its performance. The main idea of

quantum repeater is dividing the entire communication channel into many elementary links connected by nodes. QR implements steps are [38]:

- 1- Dividing the entire channel.
- 2- Creating entanglement between each two end points of elementary links.
- 3- Extending the elementary links by entanglement swapping.
- 4- Establishing the entanglement between end point of entire channel length.

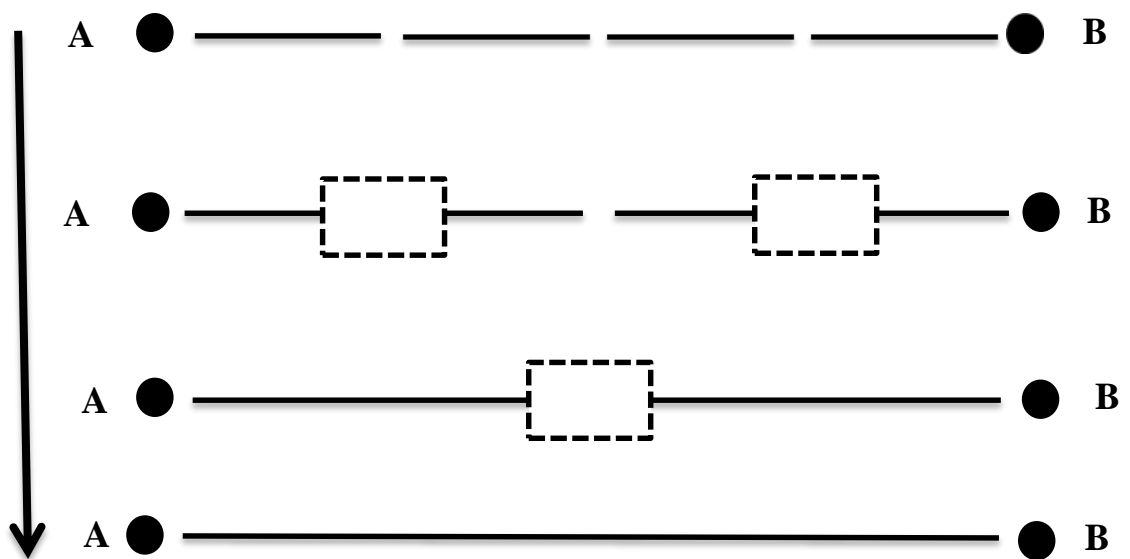


Fig. 1.8: A quantum repeater scheme implements steps.

1.6.1 Advantages of Quantum Communication vs. Classical Communication

Quantum information science and quantum communication are significant components in future quantum information processing technologies that can provide faster quantum factoring for searching data, Many of important quantum technologies are under investigation such as, QKD using single photon source to send information securely, quantum super dense coding which provides higher capacity channel and robust communications, communication complexity for higher efficiency and quantum teleportation to transmit the qubit from position to another without

physical movement. The quantum repeaters can provide a new path of disrupting entangled photon and enabling perfectly secure data transmission via global network. Altogether quantum communications schemes have in general that two or more parties are linked by both a classical communication channel and a quantum channel [39].

1.6.2 The Direct Transmission (point to point)

Point-to-point entangled photon transmission over lossy channel is limited by photon loss. The Pirandola, Laurenza, Ottaviani, and Banchi PLOB bound [40], is the upper bound on the amount of quantum information which can be sent through a lossy channel, about limited photon transmissivity η via lossy channel, is given by equation (1.54) and rates R_{PLOB} by bits per channel use per mode, for high-loss channels [40]:

$$R_{PLOB} = -\log_2 [1 - \eta] \quad (1.54)$$

Which is also a lower bound R_{PLOB} . Preceding to the discovery of the PLOB bound, the fundamental upper bound on the capacity of a *lossy* channel was known as Takeoka, Guha, and Wilde TGW, R_{TGW} [41-42]:

$$R_{TGW} = \log_2 \left[\frac{1+\eta}{1-\eta} \right] \quad (1.55)$$

Which rates by (bits per channel use per mode). This bound, derived by TGW, is denoted to as the TGW bound and is looser than the PLOB bound. Direct transmission of photons is restricted due to the exponential increase of loss in a medium, furthermore to other decoherence effects. One can try to avoid the exponential loss by sending more photonic qubits [42].

1.6.3 The Quantum No- Cloning Theorem

The no cloning theorem is an after effect of quantum mechanic that prevents the formation of indistinguishable copies of random unidentified qubits. It was expressed in 1982, besides it has significant consequences in quantum communications and associated fields. The no cloning theorem has a more important significance for the security of quantum communication protocols, and highpoints the significance of quantum teleportation for the transmission of quantum information, and this the main reason for suggesting to implement quantum repeater to distribute the entangled state between two distant locations for achieving long distance quantum communication [2] .

1.6.4 The Quantum Repeater

The main idea of most quantum repeater QR schemes is dividing an overall channel into n smaller channel links. Elementary links refer to these smaller channel segments. The fundamental upper *bound* on the quantum communication capacity of a *lossy* channel R_{PLOB} scales linearly with *transmissivity* η . The ratio of the amplitude of the electromagnetic radiation that passes through the medium. Dividing the channel into n smaller segments will allow the key rate to scale as $\eta^{1/n}$ (*where: $\eta = 10^{-\frac{L}{2L_{att}}}$, L total distance between sender and receiver, L_{att} attenuation length*), for example, photons will experience loss only in a segment of the total channel. Obviously, there must be some extra supplementary device between channel segments for the QR to function as demanded. These intermediate devices known as nodes. For each node consists of two quantum memories (QMs), there are many progresses in quantum memory of photonic entanglement by using atomic ensembles [30], also entangled photon sources presented in each node [43].

1.6.5 The Ingredients of Quantum Repeater

1.6.5.1 The Quantum Memories QMs

The long distance quantum communication through optical fibers is currently limited to a few hundreds of kilometres due to fiber losses. QRs could extend this limit to continental distances. Most approaches of QRs require highly multimode quantum memories in order to reach high communication rates. QMs play an essential role in many quantum repeater schemes, as they are needed to store intermediate quantum states between links. A QM can be defined as any physical system that can write, store, and read out a quantum state. Physical implementations often include a light-matter interface, as photonic states are read-in, stored in matter, and read-out as photonic states. However, there are many differences of QMs, here consider a QM that can generate a photonic state entangled with a state stored in the QM through some controlled mechanism, like optical pumping. Different QMs implementation will emit photons at different wavelengths [44].

If the photons generated by the QMs are not at a suitable wavelength for low-loss in a fiber, a wavelength conversion must be performed before transmission. Bell state measurements can be performed between neighboring photons by optically reading-out and entangling photonic states. The techniques for realizing such quantum memory include electromagnetically induced transparency EIT [45], far off-resonant two photon transition [46], controlled reversible inhomogeneous broadening CRIB [47], atomic frequency combs AFC [48], photon echo [49], nitrogen-vacancy (NV) centers [50], trapped atoms [51], and others [52].

1.6.5.2 Bell State Measurement BSM

To distinguish the four Bell states mentioned in equations (1.37-1.40), a Bell state measurement using linear elements such as beam splitters and single photon detectors as shown in Figure (1.9), can be used in every node of quantum repeater for creating the entanglement between each two elementary links. All elements can be described by unitary transformations. A Bell state measurement is a joint measurement on two qubits, that projects a qubits onto one of the Bell states such as in equation (1.37) [53].



Fig. 1.9: Bell State Measurement BSM. The bar is 50:50 beam splitter BS, D_1 and D_2 are detectors.

1.6.5.3 Quantum Teleportation and Entanglement Swapping

The significant resource in quantum information processing is the quantum entanglement, which enables some applications such the superdense coding [54] and the quantum teleportation [5]. Typically, entanglement can be generated in several physical systems based on second or third order nonlinear processes, some instances of entanglement generation include, the spontaneous parametric down conversion SPDC [55], the spontaneous Raman scattering SRS or spontaneous four wave mixing SFWM of atomic ensembles [56], dispersion shifted fibers DSF [57] and photonic crystal fibers PCF [58].

1.6.5.4 The Entangled Photon Sources

Entangled photon sources are essential elements of QR elements located at between each two node, required to emit photons towards the QM to establish the entanglement between QR nodes. The entangled photon sources are the key element of many quantum communication applications one of them is the QRs. A chip of single photon source SPS brings quantum communications closer as shown in Figure (1.10) [59].

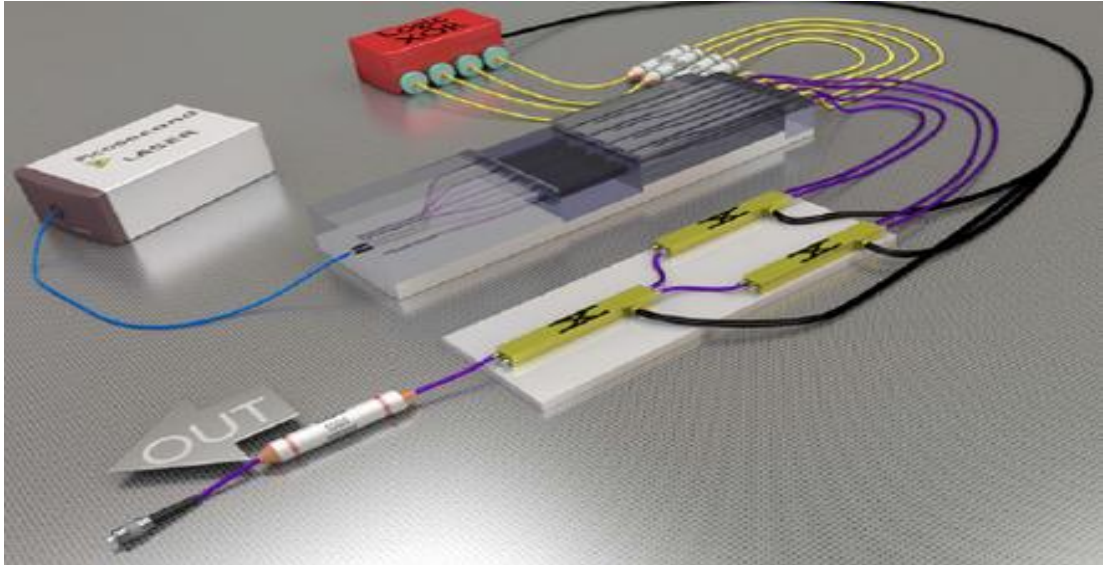


Fig. 1.10: The single photon source experimental setup [59].

The types of entangled photon sources can be used in QR scheme are:

- 1- Photon pair source PPS
- 2- Single photon source SPS

1.6.5.4.1 The QR Scheme Based on Photon Pair Source

Entangled photon pairs represent an important element in quantum information science. Entangled photon pairs is significant to be used in realization of quantum computation and quantum communications. It is needed to perform many utilities such as, entanglement swapping, quantum teleportation and linear quantum computation. The creation of entangled photon pairs could be found over parametric conversion in nonlinear optical

media [60], or using a semi-conductor quantum dot [61]. Nowadays, entangled pair sources operates with low rate, less 0.01 "pairs of photon per excitation pulse", that powerfully restrictions their applications [62]. On the other hand, the probability of a single pair of entangled photons is near unity which can emit using quantum dot, but with low extraction efficiency. The QR scheme based on PPS and MM-QM shown in Figure (1.11), but PPS is restricted by error mechanism, since even if the PPSs are perfect, the probability that two pairs will be emitted is limited by $p^2/4$ in total. Also, if one photon of pairs can be lost through its transmission through optical fiber or by detector failure and The pair-source protocols require a fixed phase relationship between the two pair sources, it will not have the desired entangled state [63] .

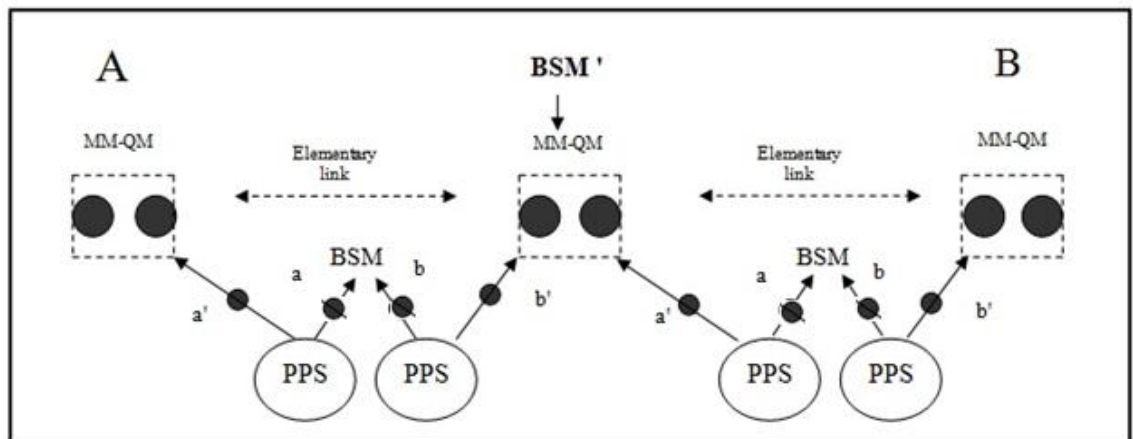


Fig. 1.11: Scheme of a quantum repeater based on multiplexing Multimode quantum memory MM-QM and photon pair source PPS. As shown BSM' performs inside nodes located between two elementary links, while BSM performs at the central station at elementary links between two nodes [63].

The procedure to entangle two remote locations A and B requires one photon-pair source and one memory at each location. The pair sources are coherently excited such that each of them can emit a pair with a small probability $p/2$, corresponding to the state [63]:

$$\left(1 + \sqrt{p/2} (a^\dagger a'^\dagger + b^\dagger b'^\dagger) + O(p)\right) |0\rangle \quad (1.56)$$

Where: a, a' and b, b' are the pairs of modes emitted by the sources located at A and B respectively, $O(p)$ is the term introduces errors in the protocol, leading to the requirement that p has to be kept small and $|0\rangle$ is the vacuum state. The modes a and b are stored in memories close to the respective sources while the modes a' and b' are sent through optical fibers to a station located half-way between A and B, where they are combined on a beam-splitter [63].

To evaluate the performance of a quantum repeater based on MM-QM and PPS, entanglement distribution rate between the endpoints (A and B) of the entire quantum channel must be calculated. Neighboring elementary links must perform entanglement swapping, including BSM' at the node of neighboring elementary links {where the prime serves to distinguish this BSM from the one performed at the center station} (see Figure (1.11)). To ensure that the elementary entanglements of neighboring links are in the same modes, a frequency conversion may be necessary before the entanglement swapping BSM' is performed, in order to have telecom wavelength. Then, if the nodes of all elementary links successfully perform a BSM' (probabilistic), entanglement is created between the end points of the quantum channel. The calculation of the probability of success of entanglement creation and entanglement distribution rate across the quantum channel is calculated as:

The probability of success of entanglement creation [63]:

$$P_{(success)} = \frac{(\eta_{mem} \eta_{d2})^{2n}}{2^{n-1}} \left(1 - \left(1 - \frac{1}{2} \eta_{d1}^2 \rho^2 10^{\frac{-\gamma L}{n}}\right)^m\right)^n \quad (1.57)$$

The entanglement distribution rate R (success), which is equal to P (success) divided by the time between successive attempts. The time between sequential attempts is given by $(w \times m) / B$ [64]. Therefore: [63]:

$$R_{success} = \frac{B}{wm} \frac{(\eta_{mem}\eta_{d2})^{2n}}{2^{n-1}} \left(1 - \left(1 - \frac{1}{2}\eta_{d1}^2 \rho^2 10^{\frac{-\gamma L}{n}}\right)^m\right)^n \quad (1.58)$$

Where:

η_{mem} is the efficiency of QM.

η_{d2} is the efficiency of the center station's detectors of BSM.

η_{d1} is detection efficiency of detectors in one node (BSM').

ρ is the probability of source to emit 1 pair of maximally entangled photons.

γ is the loss coefficient of the channel and lossy quantum channel length L.

n is the number of elementary links.

m is the number of modes emitted from QM.

B is the total bandwidth of QM.

w is the bandwidth inefficiency of QM.

1.6.5.4.2 The QR Scheme Based on Single Photon Source

The single photon source SPS can be defined as a light source that produces photons that are separated in time. This emission of photons separated in time is also known as photon anti-bunching. Nano-diamonds can be used as an emitter for single photon sources. Single photon emission systems are used in secure data transmission in quantum communication systems to prevent an unauthorized access to the data. The data is transmitted in a form of pulses of single photons. Many types of single photon source SPS has been developed, using several technologies such spontaneous

parametric down conversion SPDC, spontaneous four wave mixing SFWM, quantum dots and color centers in diamond [65].

Single photon sources SPSs are crucial elements of several future quantum technologies, It can be used for the realization of large scale quantum communications network or for connecting quantum memories in QRs as shown in Figure (1.12). The quantum communications rate scales linearly with the photon transmission via short distances, and exponentially via long distances [66].

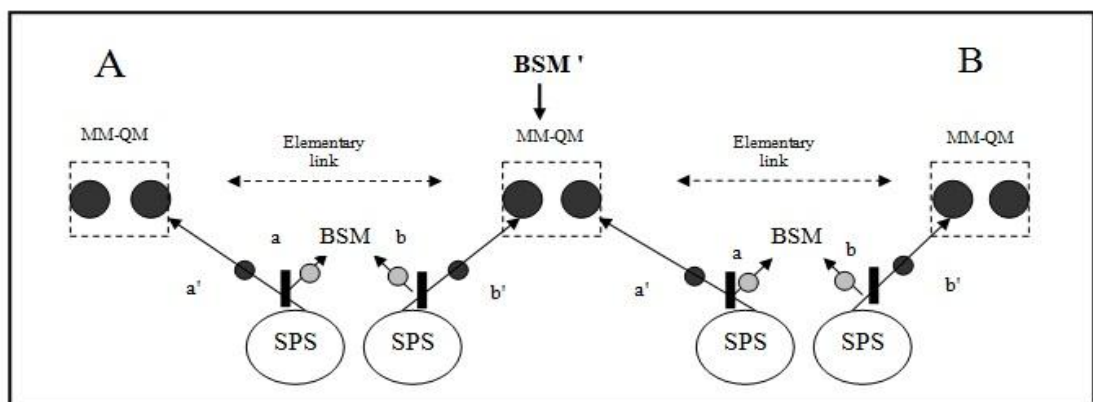


Fig. 1.12: Scheme of a quantum repeater using single photon source SPS.

Sources, memories and BSM are signified by circles. Vertical bars denote beam-splitters BS. The detection at BSM of a single photon behind the central BS projects the two memories into an entangled state [66].

The architecture of SPS scheme is represented in Figure. (1.12), the two remote locations contain each one single-photon source and one memory. When they are excited, each of the two sources ideally creates one photon. The photons created at A and B are sent through identical beam splitters with reflection and transmission coefficients $|\alpha|^2$ and $|\beta|^2$ satisfying $|\alpha|^2 + |\beta|^2 = 1$, such that after the beam-splitters, the state of the two photons is $(\alpha a^\dagger + \beta a'^\dagger)(\alpha b^\dagger + \beta b'^\dagger)|0\rangle$ which can be rewritten as [66]:

$$\alpha^2 a^\dagger b^\dagger + \alpha\beta(a'^\dagger b^\dagger + a^\dagger b'^\dagger) + \beta^2 a'^\dagger b'^\dagger)|0\rangle \quad (1.59)$$

The modes a and b are stored in memories, while the modes a' and b' are coupled into optical fibers and combined on a beam splitter at a central station, with the modes after the beam-splitter denoted by $\tilde{a} = \frac{a'+b'}{\sqrt{2}}$ and $\tilde{b} = \frac{a'-b'}{\sqrt{2}}$. The term $(a'^\dagger b^\dagger + a^\dagger b'^\dagger)|0\rangle$ may induce the detection of a single photon in mode \tilde{a} with probability $\alpha^2\beta^2\eta_t\eta_d$, where η_t is the efficiency of transmission to the central station, and η_d is the single-photon detection efficiency. For this term, the detection of a photon in \tilde{a} creates the desired state $\frac{1}{\sqrt{2}}(a^\dagger + b^\dagger)|0\rangle$ associated to entangled memories [66].

The PPS protocols require a fixed phase relationship between the two pair sources, between the $a^\dagger a'^\dagger$ and $b^\dagger b'^\dagger$ terms in eq. (1.56). There is no equivalent requirement for the SPS protocol, since the phase between the $a'^\dagger b^\dagger$ and $a^\dagger b'^\dagger$ terms in eq. (1.59) depends only on the beam-splitter transformation, and not on the phase of the pump laser. Some of PPS errors may be overcome using SPS since it is unrestricted (free) of these fundamental errors. The absence of fundamental errors proportional to the entanglement creation probability leads to very significantly improved entanglement distribution rates for the SPS protocol [66].

A quantum repeater scheme based on SPS is suggested to increase the entanglement distribution rate. Each elementary link of QR contains two SPSs and MM-QMs. When each one of the SPSs emit single photon which is split on the beam splitter into two modes, one is transmitted to store in MM-QM, or reflected the other to single photon detector SPD to perform BSM at the central station. The SPSs makes it possible to reduce errors because of two photons pair emission actions which is un-avoidable in PPS. This leads to an important improvement of the reachable entanglement distribution rate. So the SPS scheme is well-matched with the multi-mode

quantum memories MM-QMs and improved entanglement distribution rate. The performance evaluation of the suggested scheme the required total time for entanglement distribution rate is calculated [67]:

$$p(n) = (1 - P_0)^{n-1} P_0 \quad (1.60)$$

Where:

P_0 is the probability of entanglement success probability.

$$P_0 = 2p_1\beta^2\eta_t\eta_d [16].$$

η_d is the detection efficiency.

$\eta_t = \exp\left(-\frac{L_0}{2L_{att}}\right)$ is the fiber transmission efficiency.

$L_0 = \frac{L}{2^n}$ is the elementary link length.

L is entire distance

n is the elementary links number of the QR.

L_{att} is attenuation length = 22 km.

β^2 is the beam splitter transmission coefficient.

So the actual rate of entanglement creation $R(\text{success})$ of SPS can be calculated, as the reciprocal of the time between successive attempts. The time between successive attempts is given by $(w \times m) / B$ Therefore [64]:

$$R_{(\text{success SPS})} = \frac{B}{wm} p(n) \quad (1.62)$$

By using SPS with MM-QM, the entanglement distribution rate can be improved better than that with PPS.

1.6.5.4.3 Multiplexed Single Photon Source

The SPSs cannot be made to yield single photons with high probability, while at the same time defeating the probability of resulting two or more photons. As a consequence of this, single photon sources can not certainly produce single photons on request. A described multiplexed single photon source MUX-SPS as shown in Figure (2.6), system permits the probabilities of generating one and more photons to be used independently, supporting a much better estimate of an SPS on demand [68].

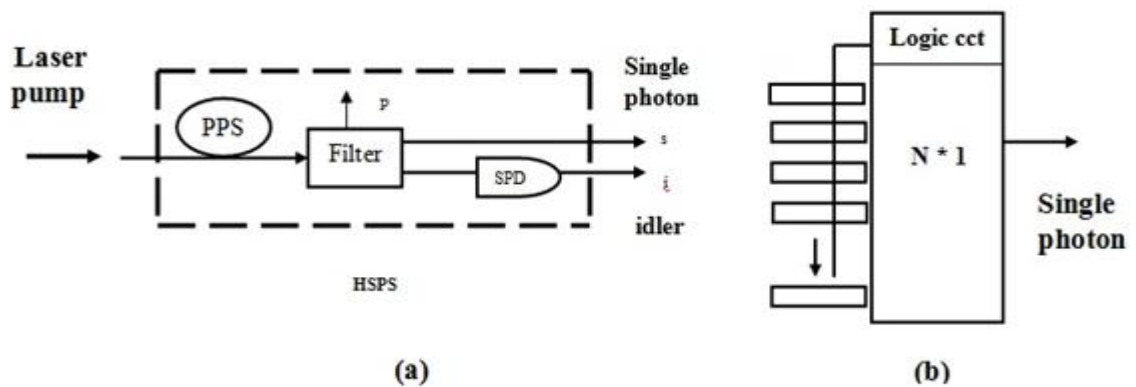


Fig. 1.13: The MUX-SPS scheme. (a) Heralded single-photon source HSPS. A laser pump of PDCS, that spontaneously emits idler and signal photons. The filter splits the laser to signal and idler. Idler photon can be detected via a single photon detector (SPD), heralding the existence of the signal photon. (b) A MUX-SPS and N HSPSs can be pumped all together, the idler photon is detected, while the signal photon is stored in a long delay line. The classical logic cct. Limits the shape for $(N \times 1)$ is detection signals switching network, routing a effectively produced to output a single photon [68].

To improve the entanglement distribution-rate of the MUX-SPS shown in Figure (1.13 (a)), two types of detectors are used, these types are threshold detector TD [69] and number-resolving detector NRD [70, 71].

1- Threshold Detector TD

For TD type, the idler arm to the trigger detector which having at least one photon probability is given by [68]:

$$P_{trigTD} = \frac{|\xi|^2 \eta_i}{1 - |\xi|^2 (1 - \eta_i)} \quad (1.63)$$

While the heralded state is a single-photon probability is [68]:

$$P_{singleTD} = (1 - |\xi|^2) \eta_s \frac{[1 - (|\xi|^2 (1 - \eta_s))^2 (1 - \eta_i)] [1 - |\xi|^2 (1 - \eta_i)]}{[1 - |\xi|^2 (1 - \eta_s)]^2 (1 - \eta_s) (1 - \eta_i)^2} \quad (1.64)$$

Where:

η_i is the idler arm efficiency.

η_s is the transmission on the signal arm efficiency.

$|\xi|^2$ is squeezing parameter of the laser source determined by the strength of the nonlinearity and the pump intensity.

2- Number Resolving Detector NRD

Now, consider the number resolving detector type, calculating one photon probability that gives as [68]:

$$P_{trigNRD} = \frac{(1 - |\xi|^2) |\xi|^2 \eta_i}{(1 - (1 - \eta_i) |\xi|^2)^2} \quad (1.65)$$

The heralded state contains one photon probability is [68]:

$$P_{singleNRD} = (1 - (1 - \eta_i) |\xi|^2)^2 \eta_s \left(\frac{(1 + (1 - \eta_i)(1 - \eta_s) |\xi|^2)}{(1 - (1 - \eta_i)(1 - \eta_s) |\xi|^2)^3} \right) \quad (1.66)$$

Furthermore, HSPSs designs are considered single-photon source SPS which has high efficiency per low multi-photons impurity if the constituent is close to perfect and NRD with 90% efficiency [70], SPS able to producing a (100 Hz) rate of (20-40) photon states with less than (10%) multi-photons impurity is probable [68]. MUX-SPS will be a valued resource for quantum technologies and quantum communications. With the high efficiency

detectors and lower loss switches, a MUX-SPS potential the threshold supplies for a completely fault-tolerant general quantum communications ought be possible. An overall MUX-SPS can be considered in a analogous technique to the HSPSs. The probability per- clock-cycle, which at least one HSPSs in an array of N-HSPSs triggers is given by [68] :

$$P_{trig}^{MUX} = 1 - (1 - P_{trig})^N \quad (1.67)$$

So, at least single source emits a triggered only one photon per clock-cycle probability is [68]:

$$P_1 = P_{single}(1 - (1 - P_{trig})^N) \quad (1.68)$$

1.6.5.4.4 Multimode Quantum memories MM-QMs

An approach for performing of quantum repeaters of the long-distance quantum communication was suggested by DLCZ in 2001 [14]. It permits to create and swap the entanglement and utilize it in the quantum teleportation. The excitation probability for generation of single photon from the atomic ensemble in QM which is used to entangle the photon emitted from an entangled photon source is small. In order to avoid multi-photon emission error occurred with excitation of a single photon in an atomic ensemble of QM for each entanglement generation attempt, long entanglement generation time is required. To eliminate this problem, multiplexing quantum memory was suggested by O. A. Collins [22] which offers higher entanglement distribution rates by MM-QM as shown in Figure (1.14).

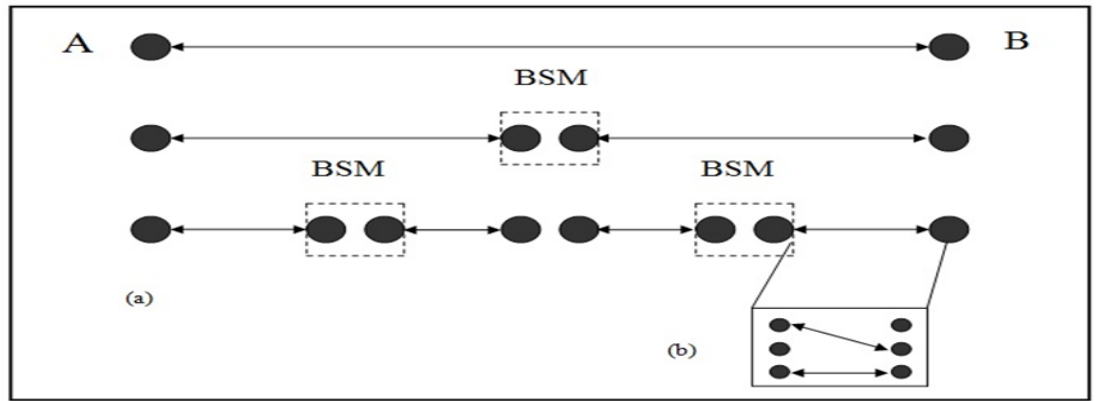


Fig. 1.14: (a) Quantum repeater scheme. (b) Multiplexing multimode quantum memory MM-QM [22].

The entanglement distribution rate in the scheme [22] measures linearly with the number of quantum memory modes utilized for multiplexing method due to higher entanglement creation probability. Though, this needs quantum memories QMs, which are able to store a greater number of modes, which could be encoded in time [72], frequency [73], or space [74]. Many multimode quantum memory MM-QM schemes are implemented such an efficient spatial multimode storage and atomic frequency comb (AFC) [75].

Distributing entangled pairs is a fundamental operation required for many quantum information science and technology tasks. The rate of entanglement distribution scheme can be increased by increasing multiplexing multimode quantum memory MM-QM number with lowering quantum memory lifetime [22].

The establishment of multiple entangled pairs can be quite challenging, especially when the parties are separated by large distances because of channel losses. An outstanding technical challenge is the long memory coherence times, motivating the exploration of methods which moderate the scaling of poor low memory. One approach is to design a system which increasing the number of trials to compensate the low success rates, by replacing single memory elements with $m > 1$ element arrays. In the multiplexed scheme as shown in Figure (1.14), the increased number of

QMs modes shows that allows for entanglement swapping and can improve the entanglement distribution rate between the terminal nodes. Now the entanglement distribution rate f_τ of m QMs modes with different memories time τ can be calculated as[22] :

$$\langle f \rangle_{\tau,n} = \frac{P_1(1-q_0^m)(1+q_0^m-2q_0^{m(\tau+1)})}{1+2q_0^m-q_0^{2m}-4q_0^{m(\tau+1)}+2q_0^{m(\tau+2)}+\delta} \quad (1.69)$$

Where:

$$\delta = \frac{q_0^{m-1}(1-q_0^m)(1-q_0^{2m-1}+2q_0^{3m-2}(1-q_0^{\tau(2m-1)}))}{(1-q_0^{2m-1})(1+q_0^m-2q_0^{(\tau+1)m})},$$

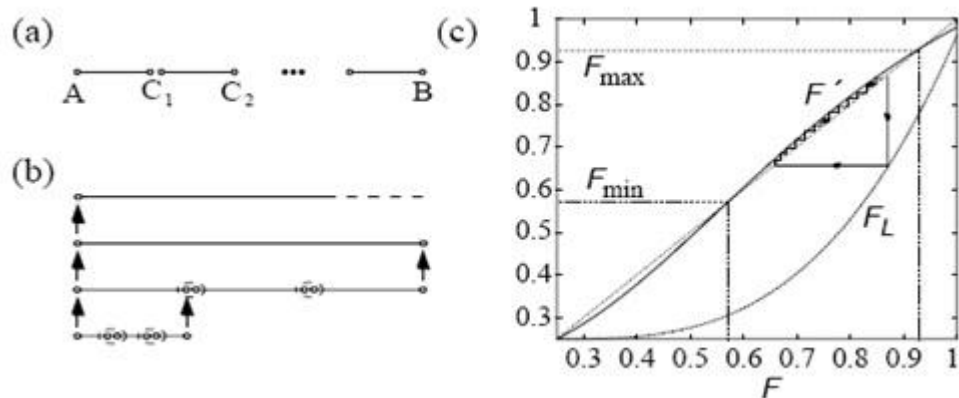
$(1 - \delta)$ is the probability of residual entanglement, P_1 is the probability of entanglement connection success, P_0 is the probability of entanglement creation, $q_0 = 1 - P_0$, m is the number of MM-QMs, and τ is QMs coherence time [22].

1.7 Literature Survey

In the following the most important research work in QR are reviewed:

1)1998- H.-J. Briegel, W. Dur, J. I. Cirac, and P. Zoller [13].

Quantum Repeaters: The Role of Imperfect Local Operations in Quantum Communication.



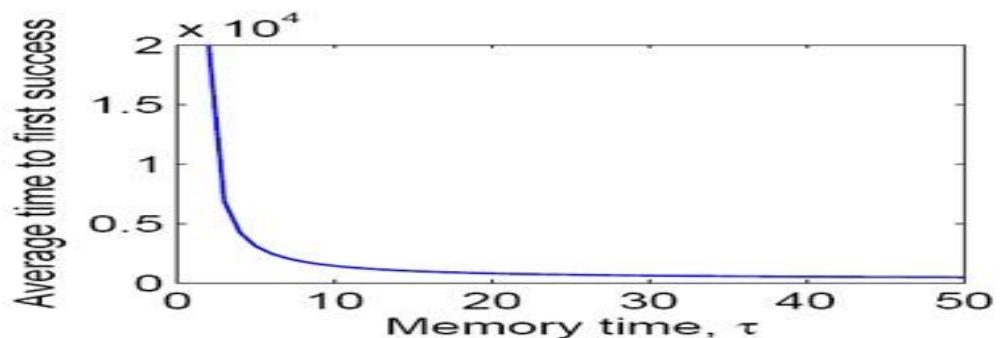
1- Fidelity of 96% over a typical “continental” (1280km).

2-The time needed to create an elementary pair = 3×10^{-4} s.

Parameters are: $L = 3, \eta = P_1 = 1, P_2 = 0.97$.

2) 2007- O.A. Collins, S.D. Jenkins, A. Kuzmich, and T.A.B. Kennedy [22].

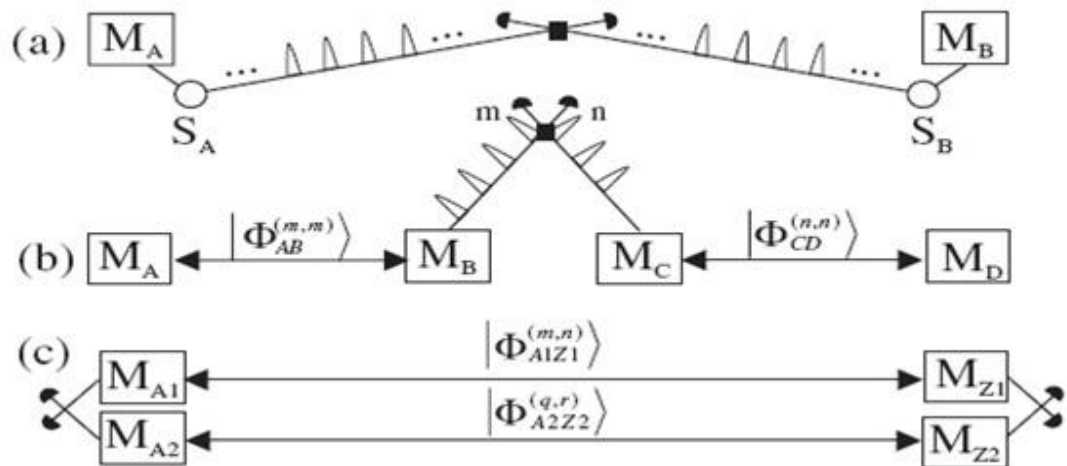
Multiplexed Memory-Insensitive Quantum Repeaters.



The entanglement distribution rate of a 1000 km reach to $\approx 10^2$ with $N = 3$ quantum repeater as a function of the quantum memory lifetime, $P_0 = 0.01$ and $P_1 = 0.5$.

3) 2007- Christoph Simon, Hugues de Riedmatten, Mikael Afzelius, Nicolas Sangouard, Hugo Zbinden, and Nicolas Gisin [63].

Quantum repeater scheme using pair sources and multimode memories.

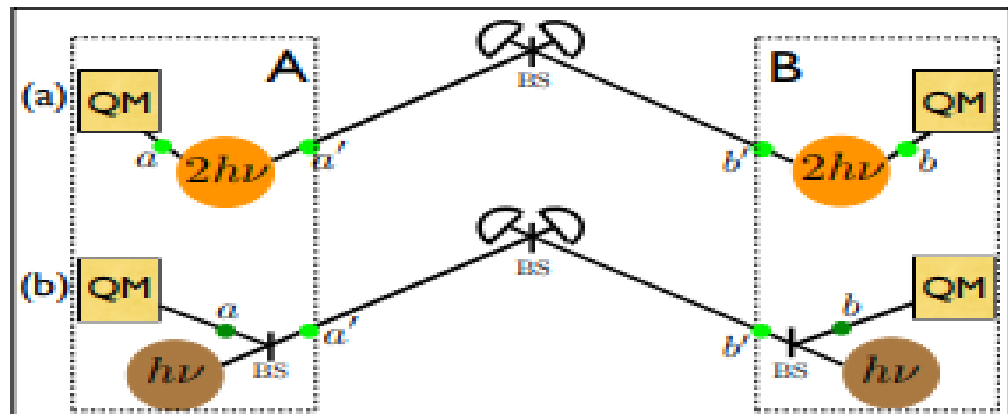


1-distance $L = 1000$ km.

2-Total time for creating entangled state = $800/N$ s, N is attempts per interval increases the success probability.

4) 2007- N. Sangouard, C. Simon, J. c. v. Min'ar, H. Zbinden, H. de Riedmatten, and N. Gisin [66].

Long-Distance Entanglement Distribution with Single-Photon Sources

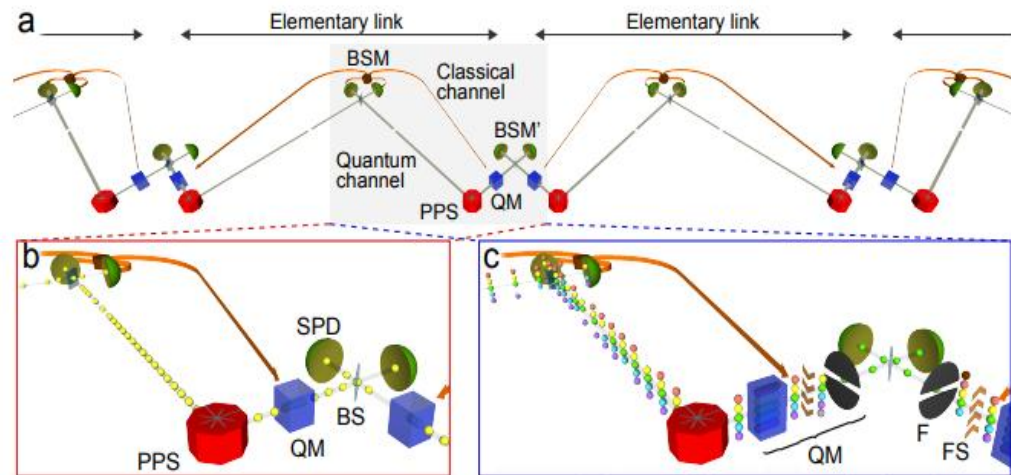


1-For PPS: $F=0.9$, $p = 0:003$ for both 1000 and 1500 km and $p = 7 \times 10^{-4}$ for both 2000 and 2500 km.

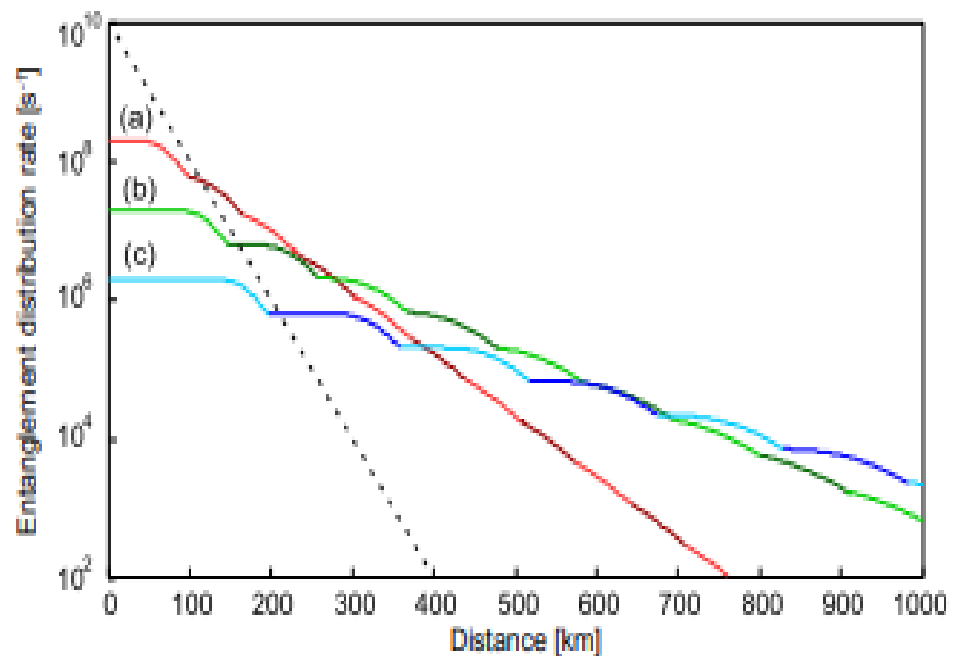
2- For SPS: $F= 0:95$, 1000 km to 2500 km.

5) 2014- N. Sinclair, E. Saglamyurek, H. Mallahzadeh, J. H. Slater, M. George, R. Ricken, M. P. Hedges, D. Oblak, C. Simon, W. Sohler [64].

Spectral multiplexing for scalable quantum photonics using an atomic frequency comb quantum memory.



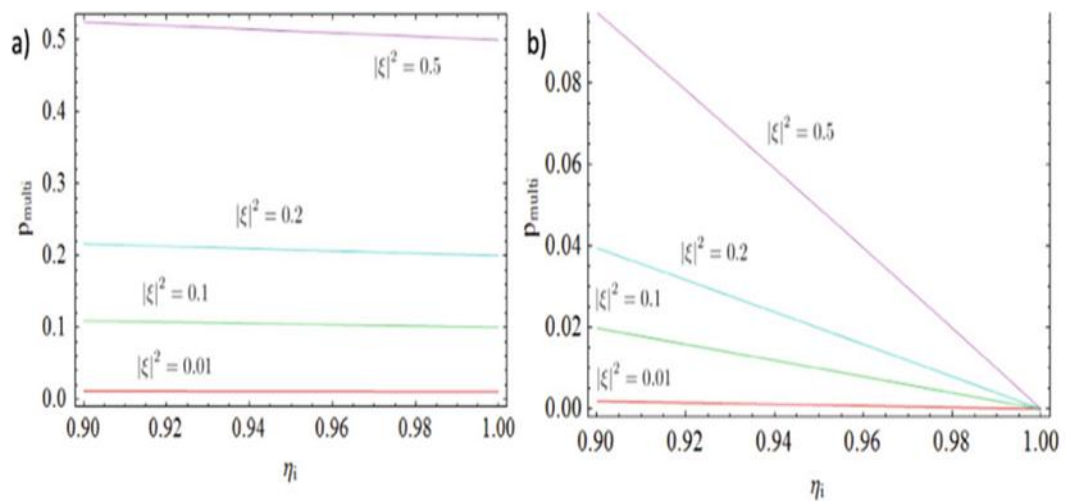
The QR scheme



Entanglement distribution rate as a function of total distance. loss of 0.2 dB/km, QMs with 90% efficiency, $B= 300$ GHz, and SPD with 90% efficiency. (a) 10^2 , (b) 10^3 , and (c) 10^4 QM modes.

6) 2015- Damien Bonneau , Gabriel J. Mendoza [12] Jeremy L. O, Brien and Mark G, Thompsony [68].

Multiplexed single-photon sources.



The Fig. shows the probability of multi-photon emission p_{multi} from a HSPS.

(a) a threshold detector, (b) a number-resolving detector.

Number-resolving detectors with 99% efficiency, a single-photon source capable of producing a 100 Hz rate of 20–40 photon states.

Chapter Two

Simulation Works

2.1 The Simulation Works

In this work, the simulation study was carried out using Python 3.7 simulation software to demonstrate that the performance of the short lifetime MM-QMs is better than the long lifetime MM-QMs contrary to the expectations. Also, do a comparison study for the performance of QR based on PPS and QR based on SPS. Then, suggesting a quantum repeater scheme based on multiplexed photon pair source MUX-PPS and QR scheme based on multiplexed single photon source MUX-SPS scheme to improve the entanglement distribution rate.

2.2 The performance of The Short Lifetime MM-QMs.

Long QM coherence times τ is an outstanding technical challenge, encouraging the investigation of methods that moderate the poor low memory scaling. The multiplexing MM-QMs is shown in Figure (1.14), found to compensate for low success rates by increasing the number of trials, and substituting a single memory element with ($m > 1$) element arrays. The increasing of m (number of QM modes) entanglement distribution rate increasing with using different τ of MM. The most important parameters in quantum storage are the decoherence times and the efficiency illustrate in table (2.1) the QM types and their lifetime and efficiencies.

Table 2.1: Summary of different quantum memory types [76].

Type	QM Efficiency η	QM lifetime τ
EIT	78%	16 s
DLCZ	73%	0.1 s
AFC	56%	20 μ s

Using equation (1.69) and table 2.1 parameter's, entanglement distribution rate of three QM types with number of quantum memory modes can be calculated.

2.3 A Comparison Study for the Performance of QR Based on PPS and QR Based on SPS

The errors presented in PPS due to low entanglement distribution rate, so to improve the entanglement distribution rate SPS can be suggested because of the SPS has less errors. Table (2.2) shows the differences between PPS and SPS.

Table 2.2: The differences between PPS and SPS.

Photon Pair Source PPS	Single Photon Source SPS
1- Low probability of photon emission ($p/2$).	1- High probability of photon emission (p).
2- High photon loss probability.	2- Low photon loss probability.
3- The PPS require a fixed phase relationship between the two pair sources, between the $a^\dagger a'^\dagger$ and $b^\dagger b'^\dagger$ terms in eq. (1.56).	3- There is no equivalent requirement for the SPS, since the phase between the $a'^\dagger b^\dagger$ and $a^\dagger b'^\dagger$ terms in eq. (1.59) depends only on the beam-splitter transformation, and not on the phase of the pump laser.

Using eq (1.62) with the parameters of table (2.3), the entanglement distribution rate of PPS and SPS with different elementary links numbers can be compared with each other.

Table 2.3: Parameters description and their values [16, 64, 66] used in the calculation (1.62) of the entanglement distribution rate of SPS-QR scheme PPS-QR.

Parameter	Parameter Description	Value
P_1	The probability that the source emits one photon	0.1
η_d	The detection efficiency	0.9
η_t	The fiber transmission efficiency	0.9
L_{att}	The attenuation length	22 km
β^2	The beam splitter transmission coefficient	0.16
B	Total bandwidth of MM-QM	300 GHz
m	The number of modes emitted from MM-QM	100 modes
w	Bandwidth inefficiency of MM- QM	10

2.4 New Approachs to Re-design The Quantum Repeater: The Suggested Schemes are:

2.4.1 QR Scheme Based on Multiplexed Photon pair Source

Active multiplexing photon pair sources MUX-PPS provides an attractive route to bypassing the problem of nondeterministic performance while retaining many of the advantages of robust. By connecting a number of sources to a network of optical switches, a photons from any one of the sources can be routed to a common output as shown in Figure (2.1)

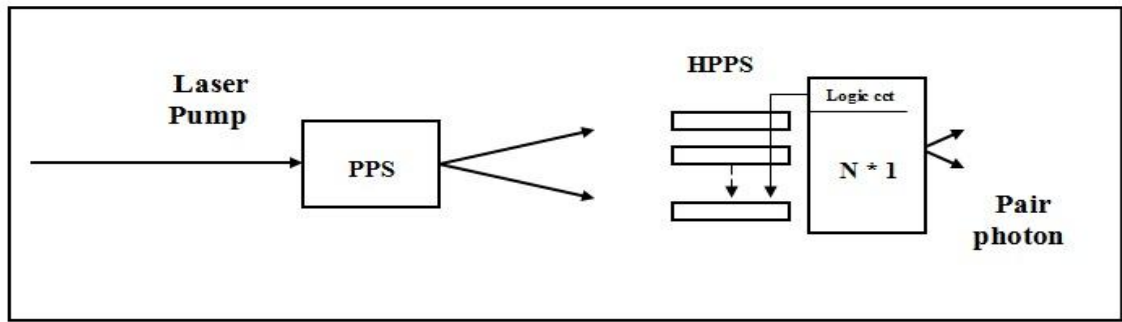


Fig. 2.1: Multiplexed photon pair source MUX-PPS.

We follow an approach based on MUX-PPS and MM-QMs which can store multiple modes at the same time. PPS suffers many mechanism errors, which can affect the entanglement distribution rate so, new scheme of quantum repeater based on multiplexed photon pair source MUX-PPS is suggested here as shown in Figure (2.2), to improve entanglement distribution rate.

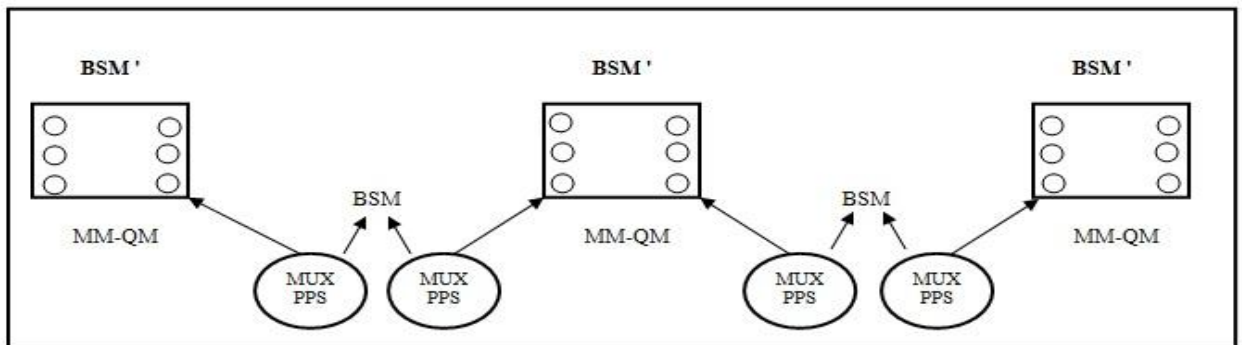


Fig. 2.2: Scheme of a quantum repeater using multiplexed photon pair source MUX-PPS-QR protocol. The circles represent MUX-PPS and the squares represent nodes contain MM-QMs. BSM' located inside node while BSM located between each two nodes.

The PPS with probability ρ emits 1 pair of maximally entangled photons and with probability $(1 - \rho)$ emits vacuum, because of inherent mechanism error in PPS, the entanglement distribution rate very low but if MUX-PPS suggesting to use, the entanglement distribution rate will slightly improve. So, for N array MUX-PPS:

$$\rho_{PPS}^{MUX} = 1 - (1 - \rho)^N \quad (2.1)$$

So, from eq (2.1) using the parameters of table (3.3) the entanglement distribution rate of MUX-PPS can be improved slightly.

Table 2.4: Parameters description and their values [63-64] used in the calculation eq (2.1) of the entanglement rate of MUX-PPS QR scheme.

Parameter	Parameter Description	Value
η_{mem}	QM efficiency	0.9
η_{d1}	Detection efficiency of detectors in one node (BSM')	0.9
η_{d2}	The efficiency of the center station's detectors of BSM	0.9
ρ	The probability of source to emit 1 pair of maximally entangled photons	0.9
α	The loss coefficient of the channel	< 0.2 dB/km
m	The number of modes emitted from MM-QM	100 modes
B	Total bandwidth of MM-QM	300 GHz
w	Bandwidth inefficiency of MM- QM	10
N	Number of MUX-PPS array	10

2.4.2 New Design of The QR Scheme Based on Multiplexed Single Photon Source

In the following is an other approach based on MUX-SPS as shown in Figure (1.13) and MM-QMs here since the entanglement distribution rate in the previous suggested scheme (MUX-PPS), has gotten slightly improvement. Since, MUX-PPS are limited by the inefficiency in emission and other errors as mentioned in chapter one .

However, the SPS is important to implement the quantum repeater to reach the longest distance. The probability of a single photon emission from a MUX-SPS is large compared to the probability of a photon emission from SPS. So, for higher entanglement distribution rate with longer distances, QR based on MUX-SPSs with MM-QMs suggested here as shown in see Figure (2.3).

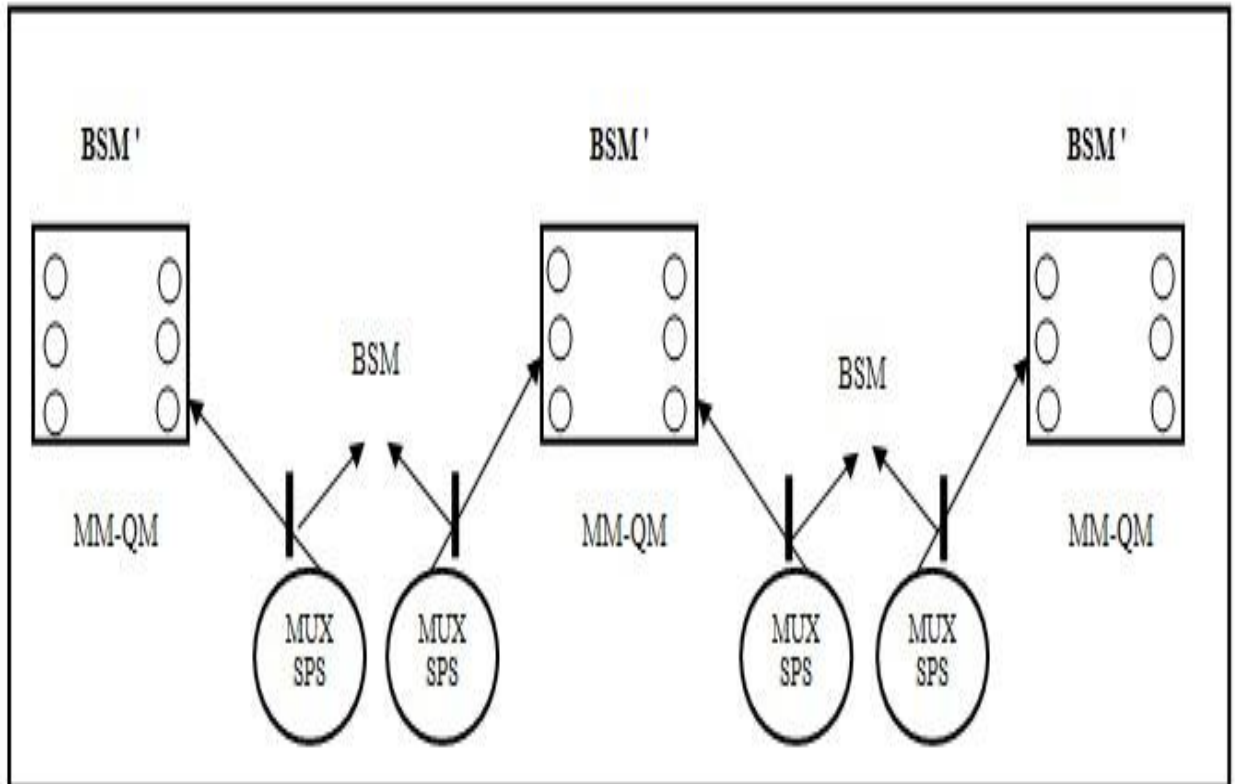


Fig. 2.3: Suggested scheme of QR uses MM-QM in combination with MUX-SPS.

The circles represent MUX-PPS and the squares represent nodes contain MM-QMs. BSM' located inside node while BSM located between each two nodes. Bars represent Beam splitter BS.

The entanglement distribution rate from eq (1.68) with other equations of TD (1.63), (1.64) and equations of NRD (1.65), (1.66), and using parameters of table (2.5) can be calculated.

Table 2.5: Parameters description and their values [64], [66] used in the calculation equations (1.64, 1.66, 1.68) of the entanglement distribution rate of MUX-SPS-QR scheme.

Parameter	Parameter Description	Value
η_d	The detection efficiency	0.9
η_t	The fiber transmission efficiency	0.9
L_{att}	The attenuation length	22 km
η	The total efficiency	$\eta_d \eta_t$
β^2	The beam splitter transmission coefficient	0.16
c	Speed of light in optical fiber	2×10^8 m/s
B	Total bandwidth of MM-QM	300 GHz
m	The number of modes emitted from MM-QM	100 modes
w	Bandwidth inefficiency of MM- QM	10
η_i	The idler arm efficiency	0.9
η_s	The signal arm efficiency	0.9
$ \xi ^2$	Squeezing parameter of the laser source	0.5
N	Number of MUX-SPS array	10

Depending on type of detector of HSPSs of Fig. 2.7 (a) the probability to produce single photon P_1 of the MUX-SPS illustrated in Fig. 6 (b) will be increased, by calculating eq (1.68) with eq $P_0 = 2p_1\beta^2\eta_t\eta_d$, then entanglement distribution rate of MUX-SPS can be calculated from eq (1.60). These calculations show the increasing of entanglement distribution rate for QR scheme based on MUX-SPS higher than that by using SPS as it is shown in following section. Also, higher improvement of entanglement distribution rate of MUX-SPS is achieved using NRD which has a higher photon detecting efficiency than a TD.

Chapter Three

Results, Discussion,

Conclusion and Future

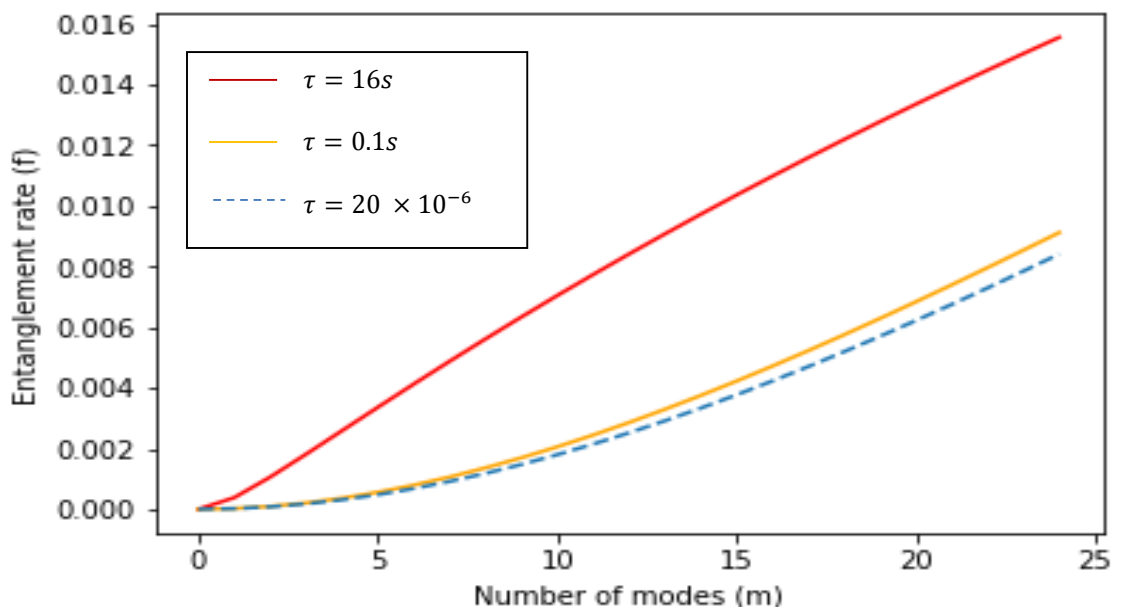
Work

3.1 Introduction

The improvement of the entanglement distribution rate between remotely located nodes of the quantum repeater is a challenge. This rate has been primarily limited by the small probability for successfully entanglement swapping success. In this chapter, the results of entanglement distribution rate of the suggested QR schemes based on MUX-PPS, SPS and MUX-SPS all in combination with MM-QR.

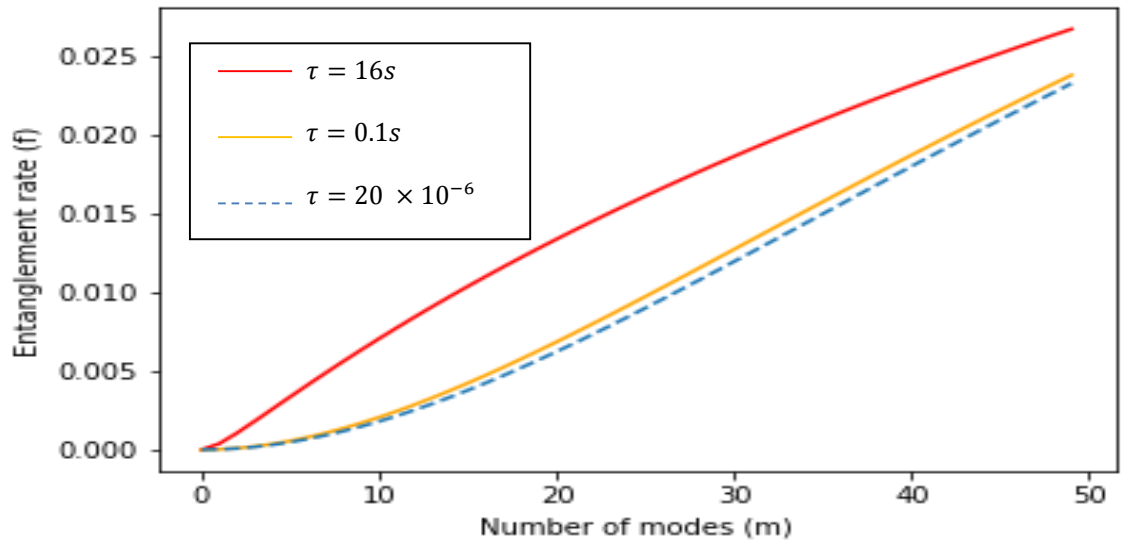
3.2 The Relationship of Lifetime MM-QM with Entanglement Rate

In this section, referring to (1.69) the entanglement distribution rate for different values of MM-QMs lifetimes with different values of a number of modes ($m = 25, 50, 100, 500 \text{ modes}$) is shown in Figure (3.1. (a, b, c, d)) and in table (3.1).

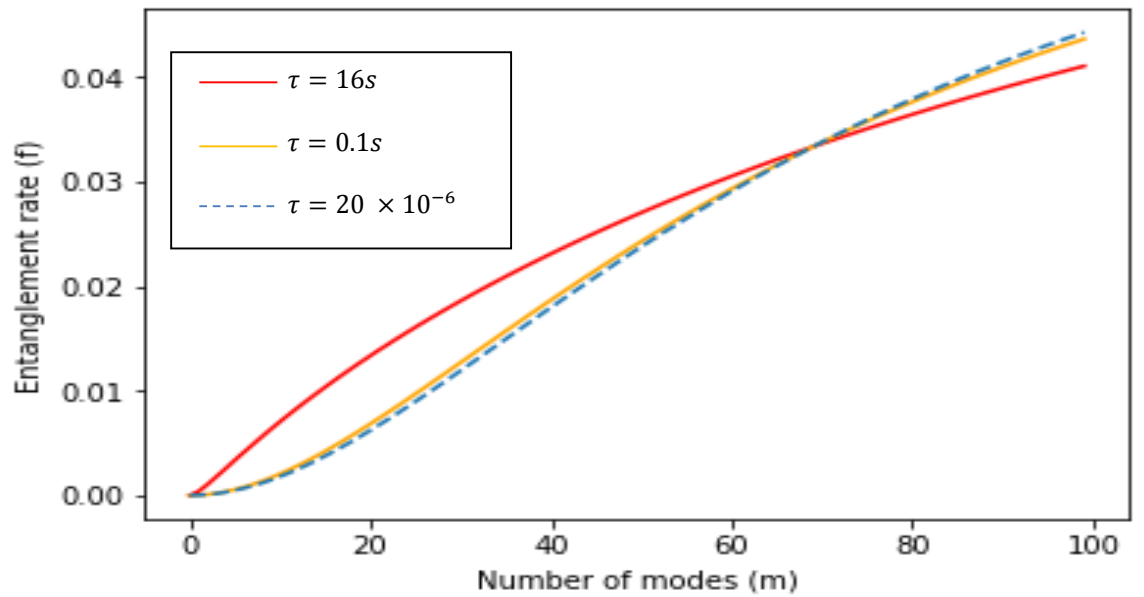


(a)

Fig. 3.1: The entanglement distribution rate of MM-QMs with different QM times, $P_0 = 0.01, P_1 = 0.5$ red line of $\tau = 16s$, orange line of $\tau = 0.1s$, dashed line of $\tau = 20 \times 10^{-6}s$, (a) $m = 25$, (b) $m = 50$, (c) $m = 100$, (d) $m = 500$.

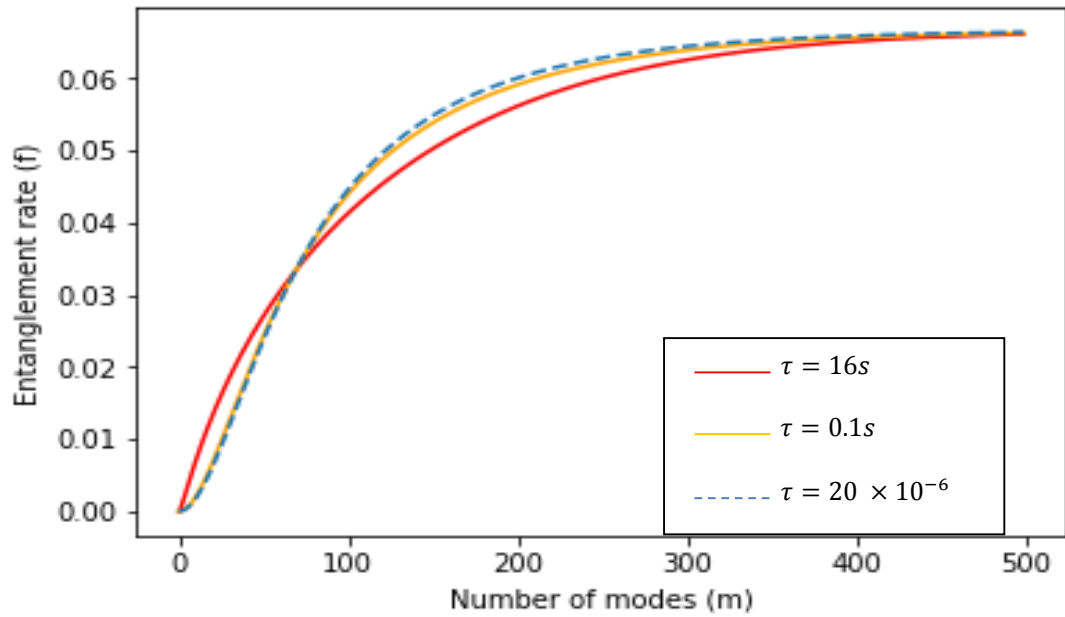


(b)



(c)

Fig. 3.1: The entanglement distribution rate of MM-QMs with different QM times, $P_0 = 0.01, P_1 = 0.5$ red line of $\tau = 16\text{ s}$, orange line of $\tau = 0.1\text{ s}$, dashed line of $\tau = 20 \times 10^{-6}\text{ s}$, (a) $m = 25$, (b) $m = 50$, (c) $m = 100$, (d) $m = 500$.



(d)

Fig. 3.1: The entanglement distribution rate of MM-QMs with different QM times, $P_0 = 0.01, P_1 = 0.5$ red line of $\tau = 16s$, orange line of $\tau = 0.1s$, dashed line of $\tau = 20 \times 10^{-6}s$, (a) $m = 25$, (b) $m = 50$, (c) $m = 100$, (d) $m = 500$.

Table 3.1:The entanglement distribution rate values with different quantum memories lifetime τ and different numbers of modes m .

QM Modes m	The Entanglement Distribution Rate (1/s) of $\tau_1=16s$	The Entanglement Distribution Rate (1/s) of $\tau_2=0.1s$	The Entanglement Distribution Rate (1/s) of $\tau_3=20 \times 10^{-6}s$
25	0.015	0.008	0.006
50	0.026	0.024	0.023
100	0.04	0.049	0.05
500	0.06	0.06	0.06

3.3 The Entanglement Distribution Rate of QR Scheme Based on MUX-PPS

Next, referring to eq (2.1) the entanglement distribution rate using the parameters of table (2.4) of QR based on MUX-PPS with elementary links $n = 3$ shown in Figure. (3.2) and estimated results in table .

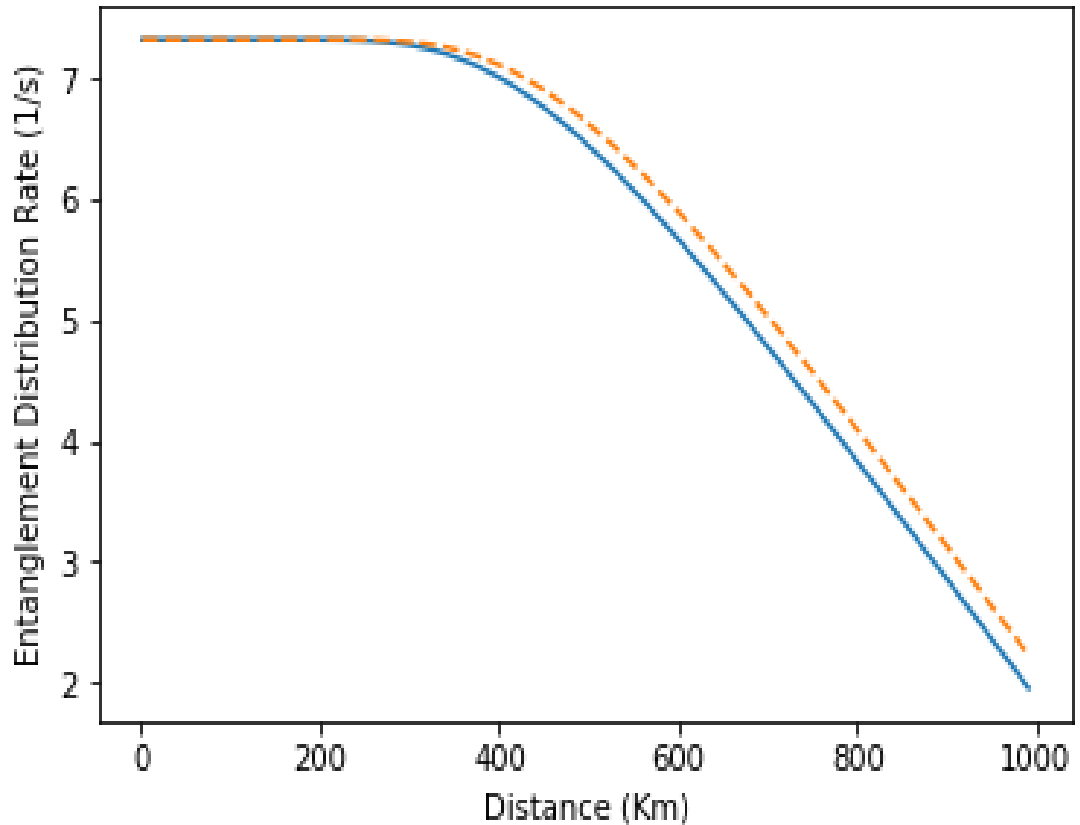
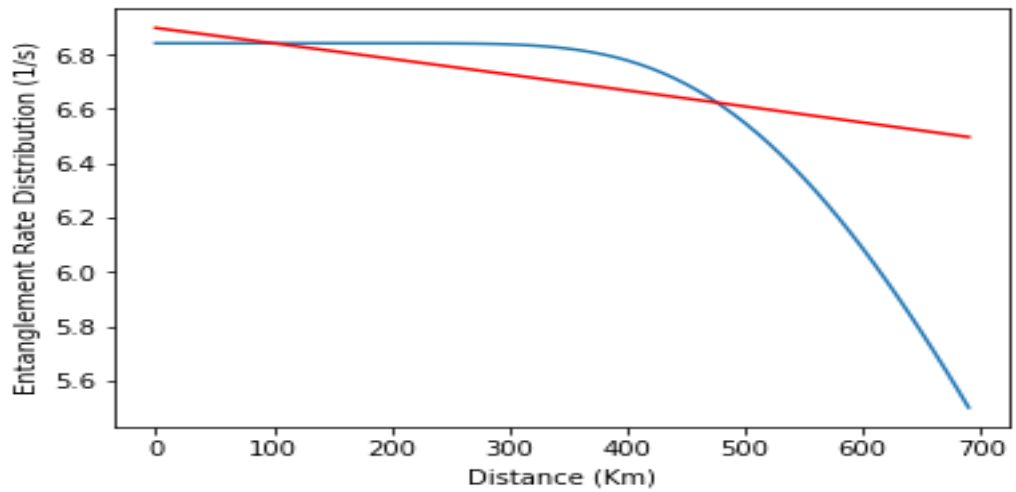


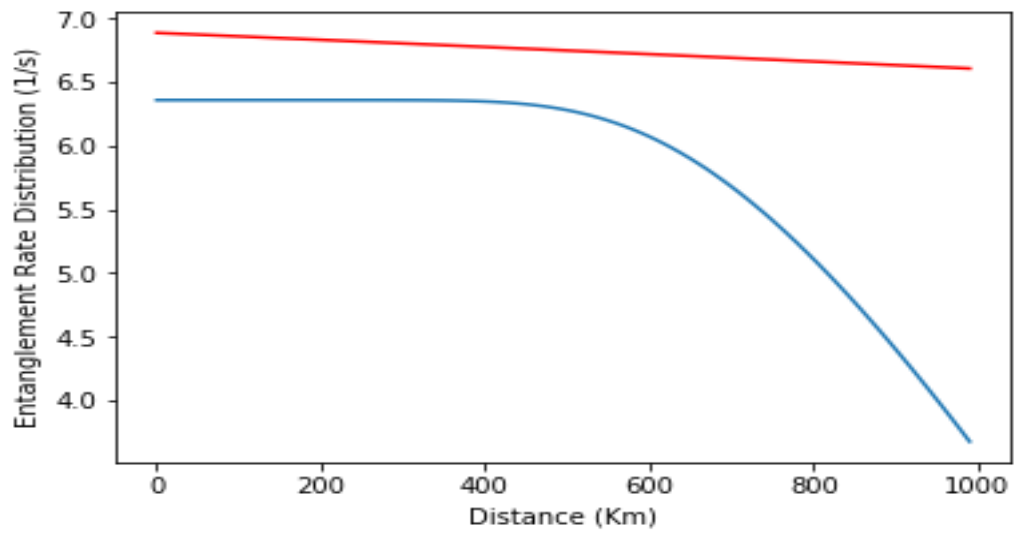
Fig. 3.2: The entanglement distribution rate of QR scheme based on MUX-PPS. (Blue line) of PPS, (Dashed line) of MUX-PPS, $n = 3$.

3.4 The Entanglement Distribution Rate of QR Scheme Based on SPS

Referring to eq (1.60) the entanglement distribution rate using the parameters of table (2.3) of QR based on SPS with elementary links ($n = 4, n = 5$) has been calculated as shown in Figure. (3.3 a and b) and table (3.2).



(a)



(b)

Fig. 3.3: The entanglement distribution rate of QR scheme based on SPS. (Red line) of SPS, (Blue line) of PPS, (a) $n = 4$, (b) $n = 5$.

Table 3.2: The entanglement distribution rate comparison results between PPS-QR and SPS-QR.

Distance (km)	The PPS-QR Entanglement distribution Rate (1/s)	The SPS-QR Entanglement distribution Rate (1/s)
700	7.3	6.8
1000	6.3	7

3.5 The Entanglement Distribution Rate of QR Scheme Based on MUX-SPS

From the calculations of single photon emission probability eq (1.68) of MUX-SPS with eq (1.68), the entanglement distribution rate can be calculated from eq (1.62), more improvement of entanglement distribution rate for MUX-SPS quantum repeater scheme can be shown in Figure (3.4) with elementary links ($n = 3$) and table (3.3).

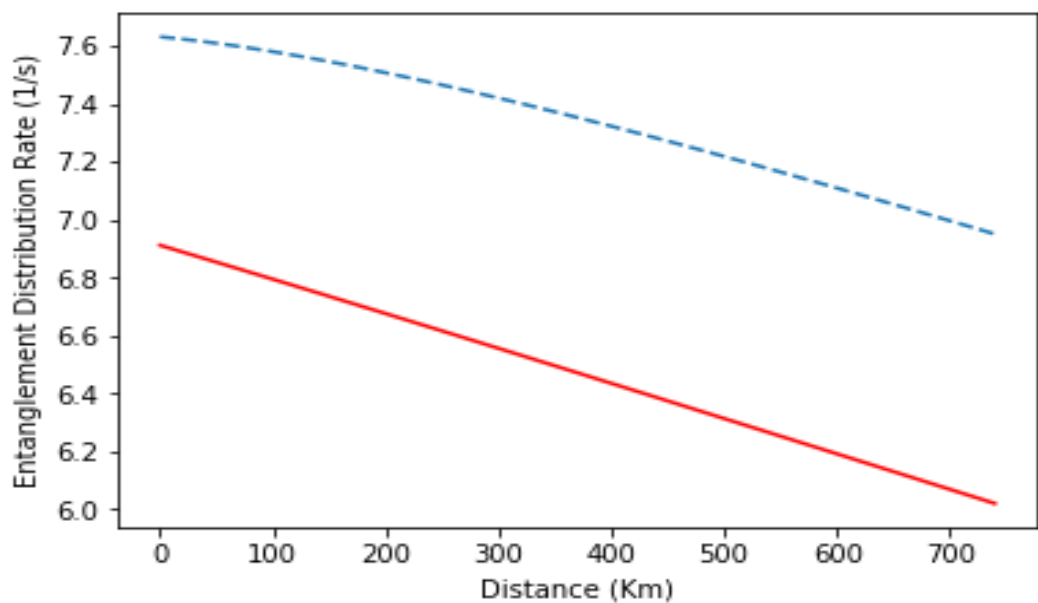


Fig. 3.4: The entanglement distribution rate of QR scheme based on MUX-SPS and SPS. (Dashed line) of MUX-SPS, (Red line) of SPS, with $n = 3$.

Table 3.3: The entanglement distribution rate comparison results between SPS-QR and MUX-SPS-QR.

Distance (km)	The SPS-QR Entanglement distribution Rate (1/s)	The MUX-SPS-QR Entanglement distribution Rate (1/s)
700	6.9	7.8

Also, From the calculations of single photon emission probability eq (1.68) of MUX-SPS parameter's of TD eq.s (1.63-1.64) and NRD eq.s (1.65-1.66) with eq (1.68), the entanglement distribution rate can be calculated from eq (1.62), improvement of entanglement distribution rate for MUX-SPS with NRD parameter quantum repeater scheme can be shown in Figure (3.5) with elementary links ($n = 3$) and table (3.4).

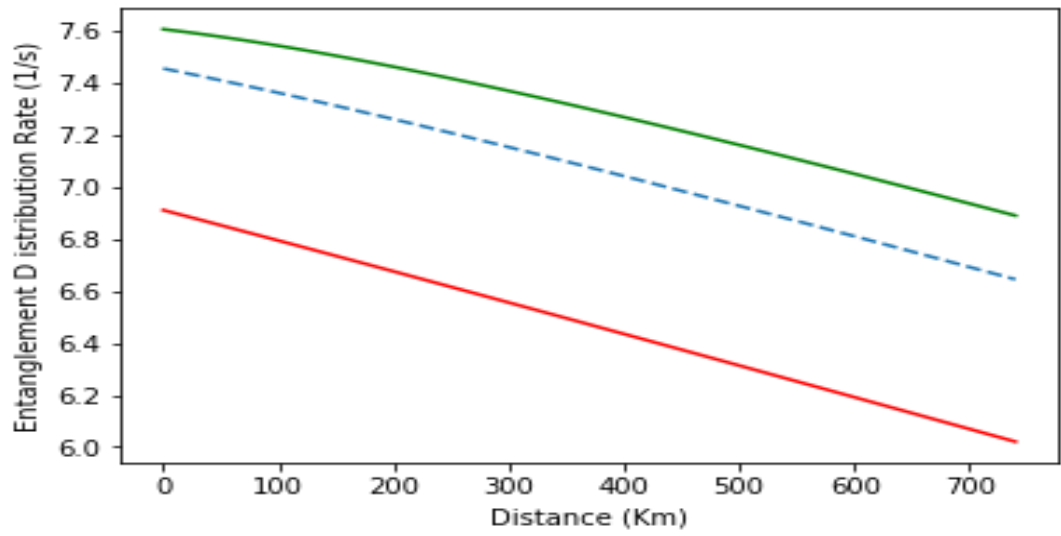


Fig. 3.5: The entanglement distribution rate of QR scheme based on MUX-SPS and SPS. (Green line) of MUX-SPS with NRD, (Dashed line) of MUX-SPS with TD, (Red line) of SPS, with $n = 3$.

Table 3.4: The entanglement distribution rate comparison results between SPS-QR and MUX-SPS-QR.

Distance (km)	The SPS-QR Entanglement distribution Rate (1/s)	The MUX (TD)-SPS-QR Entanglement distribution Rate (1/s)	The MUX(NRD)-SPS-QR Entanglement distribution Rate (1/s)
700	6.9	7.5	7.8

So, the simulation results show that the quantum repeater scheme based on multiplexed single photon source MUX-SPS can achieve an improvement

at an entanglement distribution rate created between sender and receiver with long distance quantum communication with a secure message transmission.

3.6 Discussion

The slightly improvement of entanglement distribution rate for MUX-PPS-QR makes the MUX-PPS ineffective for long distances. So, the SPS is more suitable for long distances while PPS is more suitable for short distances.

On the other side, the MUX-SPS-QR give higher entanglement distribution rate than SPS-QR since MUX-SPS that has higher single photon emission probability than the SPS.

However, the short lifetime MM-QMs with higher number modes can give higher entanglement distribution rate since a multiplexing of quantum nodes are largely insensitive to the coherence times τ of the quantum memory elements. But on the other hand, this requires a high cost of implementation.

3.7 Conclusion

In this work, it's obvious from Figure (3.1. 2c & 2d), that at the high number of QMs modes ($m > 40$ modes), the improvement of the entanglement distribution rate is gotten by using short lifetime MM-QMs more than that with long lifetime MM-QMs, so the quantum channel can be extended. These findings are a consequence from the fact that with higher number of MM-QMs modes, the long lifetime MM-QMs will enhance more residual entangled photon pairs which reduce the rate of entanglement distribution.

While for low number of MM-QMs modes at quantum repeater nodes, long lifetime MM-QMs show higher entanglement distribution rate than that using short lifetime MM-QMs as shown in Figure (3.1. 2a &2b). This achievement in combination with the effect of decoherence, low efficiencies and the difficulties of long lifetime MM-QMs fabrication make the multiplexed quantum repeater scheme with short lifetime MM-QMs more reliable.

However, the MUX-PPS has higher photon emitting probability than that PPS, so the Figure (3.2) shows the entanglement distribution rate of MUX-PPS quantum repeater scheme exceeded the entanglement distribution rate of the quantum repeater scheme based on PPS.

As shown in Figure (3.3) the entanglement distribution rate of SPS outperforms on the entanglement distribution rate of PPS and these results are likely expected since SPS free of errors which PPS suffered from. Consequently, the long distances quantum channel is achieved by SPS scheme. Furthermore, the higher entanglement distribution rate using the MUX-SPS is satisfied as shown in Figure (3.4) and Figure (3.5) taking into consideration the NRD which has a high efficiency detection. The advantage of using such a method is reducing the needed to higher waiting time for creating an entangled pair, Then it will reduce the detrimental effects of the decoherence effect on the quantum memories in use. With these improvements a quantum repeater may become realistically achievable in the near term.

3.8 Future Work

- ❖ Study the possibility of using different types of quantum memories (Non identical quantum memories) if can be used in the same MUX-SPS quantum repeater suggested scheme for more entanglement distribution rate improvement.

- ❖ Calculate the fidelity of the quantum repeater scheme using MUX-SPS and compare it with other quantum repeater schemes.

References

References

- [1] P. Zoller, Th. Beth, D. Binosi, R. Blatt, H. Briegel, "Quantum information processing and communication", *Eur. Phys. J. D* 36, 203–228, DOI: 10.1140/epjd/e2005-00251-1, (2005).
- [2] William K. Wootters and Wojciech H. Zurek. The no-cloning theorem. American Institute of Physics, S-0031-9228-0902-350-3,(2009).
- [3] V. Scarani, H. Bechmann-Pasquinucci, N. J. Cerf, M. Dušek, N. Lu'tkenhaus, and M. Peev. The security of practical quantum key distribution. *Rev. Mod. Phys.*, 81:1301–1350, (2009).
- [4] H. -L. Yin. Measurement-device-independent quantum key distribution over a 404 km optical fiber. *Phys. Rev. Lett.*, 117:190501, (2016).
- [5] C. H. Bennett et al., "Teleporting an unknown quantum state via dual classical and Einstein-Podolsky-Rosen channels", *Phys. Rev. Lett.* 70, 1895 (1993).
- [6] P. Kok et al., "Linear optical quantum computing with photonic qubits", *Rev. Mod. Phys.* 79, 135 (2007).
- [7] R. Blatt and D. J. Wineland, "Entangled states of trapped atomic ions", *Nature* 453, 1008 (2008).
- [8] J. Clarke and F. K. Wilhelm, "Superconducting quantum bits", *Nature* 453, 1031 (2008).
- [9] H. J. Kimble, "The quantum internet", *Nature* 453, 1023 (2008).
- [10] I. Bloch, "Quantum coherence and entanglement with ultracold atoms in optical lattices", *Nature* 453, 1016 (2008).
- [11] J. S. Bell, "On the Einstein Podolsky Rosen paradox", *Physics* 1, 195 (1964).

- [12] R. Ursin et al., "Entanglement-based quantum communication over 144 km", *Nature Physics* 3, 481 (2007).
- [13] H.-J. Briegel, W. Dur, J. I. Cirac, and P. Zoller, "Quantum Repeaters: The Role of Imperfect Local Operations in Quantum Communication", *Phys. Rev. Lett.* 81, 5932 (1998).
- [14] D. Lukin, L.-M. Duan, M., J. I. Cirac, and P. Zoller, "Long-distance quantum communication with atomic ensembles and linear optics", *Nature* 414, 413 (2001).
- [15] SU XiaoLong, JIA XiaoJun, XIE ChangDe & PENG KunChi. *Sci China-Phys Mech Astron*, 10.1007/s11433-013-5358-0, (2014).
- [16] Sangouard, N., Simon, C., de Riedmatten, N. & Gisin, N. Quantum repeaters based on atomic ensembles and linear optics. *Rev. Mod. Phys.* 83,33–80 (2011).
- [17] Grudka, A. et al. Long-distance quantum communication over noisy networks without long-time quantum memory. *Phys. Rev. A* 90, 062311 (2015).
- [18] Koji Azuma, Kiyoshi Tamaki & Hoi-Kwong Lo, *Nature Communications*, 6:6787, DOI: 10.1038/ncomms7787, (2015).
- [19] Silvestre Abruzzo, Sylvia Bratzik, Nadja K Bernardes, Hermann Kampermann, Peter van Loock, and Dagmar Bru. arXiv:1208.2201v2 [quant-ph] 18 Jun (2013).
- [20] De Riedmatten, H. et al. Long-distance entanglement swapping with photons from separated sources. *Phys. Rev. A* 71, 050302 (2005).
- [21] David Edward Bruschi, Thomas M. Barlow, Mohsen Razavi, and Almut Beige, "Repeat-until-success quantum repeaters", arXiv:1407.3362v1 [quant-ph] 12 Jul, (2014).
- [22] O.A. Collins, S.D. Jenkins, A. Kuzmich, and T.A.B. Kennedy, *Phys. Rev. Lett.* 98, 060502 (2007).

- [23] S.A. Rashkovskiy Institute for Problems in Mechanics, Russian Academy of Sciences, Vernadskogo Ave., 101/1 Moscow, 119526, (2013).
- [24] S Imre, L Gyongyosi, "Advanced Quantum Communications" An Engineering Approach. Institute of Electrical and Electronics Engineers. United States of America. (2012).
- [25] K. Purbhoo, "Notes on Tensor Products and the Exterior Algebra For Math 245" (2012).
- [26] Michael A. Nielsen and Isaac L. Chuang. Quantum Computation and Quantum Information. Cambridge University Press, (2000).
- [27] Giuliano Benenti, Giulio Casati and Giuliano Strini, " Principles of Quantum Computation and Information" , World Scientific Publishing Co. Pte. Ltd, (2004).
- [28] Eleanor Rieffel and Wolfgang Polak " Quantum Computing" ,Massachusetts Institute of Technology, QA76.889.R54, (2011).
- [29] Joan Vaccaro. Quantum Computer Simulator, griffith.edu.au/joan/index.php (2013).
- [30] Olivier Gazzano and Glenns S. Solomon, " Toward optical quantum information processing with quantum dots coupled to microstructures", Vol. 33, No. 7 / Journal of the Optical Society of America B, (2016).
- [31] Gregg Jaeger, "Bell Gems: the Bell basis generalized", arXiv:quant-ph/0407251v1, (2004).
- [32] M. B. Russell, L. O. Mailloux, D. D. Hodson, M. R. Grimaila, " A Bell State Analyzer Model for Measurement Device Independent Quantum Key Distribution" Int'l Conf. Scientific Computing , (2017).
- [33] John P. Hayes, " Basic Concepts in Quantum Circuits " Advanced Computer Architecture Laboratory EECS Department University of Michigan, Ann Arbor, MI 48109, 9USA, (2003).

- [34] Sören Wengerowsky, Siddarth Koduru Joshi, Fabian Steinlechner, Hannes Hübel and Rupert Ursin, "An entanglement-based wavelength-multiplexed quantum communication network", *Nature* volume 564, pages 225–228, (2018).
- [35] Li-Nan Jiang, "Quantum Teleportation Under Different Collective Noise Environment" *International Journal of Theoretical Physics* (2018).
- [36] Christian Mastromattei "Assessing the Practicality of a Simple Multi-node Quantum Repeater" A thesis presented to the University of Waterloo in fulfillment of the thesis requirement for the degree of Master of Science in Physics, (2017).
- [37] Aeysha Khalique and Barry C. Sanders, " Long-distance quantum key distribution using concatenated entanglement swapping with practical resources", *Optical Engineering* 56(1), 016114 (2017).
- [38] Takahiko Satoh, Shota Nagayama, Takafumi Oka and Rodney Van Meter, " The Network Impact of Hijacking a Quantum Repeater" arXiv:1701.04587v4 [quant-ph] (2018).
- [39] Robert J. Runser, Thomas Chapuran, Paul Toliver, Nicholas A. Peters, Matthew S. Goodman, Jon T. Kosloski, Nnake Nweke, Scott R. McNown, Richard J. Hughes, Danna Rosenberg, Charles G. Peterson, Kevin P. McCabe, Jane E. Nordholt, Kush Tyagi, Philip A. Hiskett, Nicholas Dallmann. Telcordia Technologies, 331 Newman Springs Rd., Red Bank, NJ 07701. (2015).
- [40] S. Pirandola, R. Laurenza, C. Ottaviani, and L. Banchi. Fundamental limits of repeaterless quantum communications. *Nature Communications*, 8:15043, Apr (2017).
- [41] D. Luong, L. Jiang, J. Kim, and N. Lutkenhaus. Overcoming lossy channel bounds using a single quantum repeater node. *Applied Physics B*, 122(4):96, Apr (2016).

- [42] M. Takeoka, S. Guha, and M. M. Wilde. The squashed entanglement of a quantum channel. *IEEE Transactions on Information Theory*, 60(8):4987{4998, Aug} (2014).
- [43] Rodney Van Meter, Thaddeus D. Ladd, W.J. Munro, and Kae Nemoto, "System Design for a Long-Line Quantum Repeater", arXiv:0705.4128v2 [quant-ph] (2008).
- [44] Mikael Afzelius, Nicolas Gisin, and Hugues de Riedmatten, "Quantum memory for photons", *Physics Today*, (2015).
- [45] T. Chanelière, D. N. Matsukevich, S. D. Jenkins, S.Y. Lan, T. A. B. Kennedy & A. Kuzmich. Storage and retrieval of single photons transmitted between remote quantum memories. *Nature*, 438,833,836, (2005).
- [46] Dong Sheng Ding, Wei Zhang, Zhi Yuan Zhou, Shuai Shi ,Guo Yong Xiang, Xi Shi Wang, Yun Kun , Jiang Bao, Sen Shi, Guang Can Guo. Quantum Storage of Orbital Angular Momentum Entanglement in an Atomic Ensemble. arXiv:1404.0439 (2014).
- [47] W. Tittel, M. Afzelius, T. Chanelière, R.L. Cone, S. Kröll, S.A. Moiseev, M. Sellars. Photon-echo quantum memory in solid state systems. *Laser Photon. Rev.*4, 244 (2010).
- [48] Christoph Clausen, Imam Usmani, Félix Bussièrès, Nicolas Sangouard, Mikael Afzelius, Hugues de Riedmatten, Nicolas Gisin, Quantum storage of photonic entanglement in a crystal. *Nature*.469,508.511(2011).
- [49] Hosseini, M., Sparkes, B. M., Campbell, G., Lam, P. K. & Buchler, B. C. High efficiency coherent optical memory with warm rubidium vapour. *Nat. Commun.* 2, 174 (2011).
- [50] S. E. Vinay and P. Kok. Practical repeaters for ultralong-distance quantum communication. *Phys. Rev. A*, 95:052336, May (2017).
- [51] T. P. Harty, D. T. C. Allcock, C. J. Ballance, L. Guidoni, H. A. Janacek, N. M. Linke, D. N. Stacey, and D. M. Lucas. High-fidelity

preparation, gates, memory, and readout of a trapped-ion quantum bit. *Phys. Rev. Lett.*, 113:220501, Nov (2014).

- [52] J. Borregaard, P. Kómár, E. M. Kessler, M. D. Lukin, and A. S. Sørensen. Long-distance entanglement distribution using individual atoms in optical cavities. American Physical Society. *PHYSICAL REVIEW A* 92, 012307 (2015).
- [53] Yoon-Ho Kim, Sergei P. Kulik, and Yanhua Shih." Quantum Teleportation with a Complete Bell State Measurement", PACS Number: 03.65.Bz, 03.67.Hk, 42.50.Dv, 42.65.Ky (2003).
- [54] K. Mattle, H. Weinfurter, P. G. Kwiat, and A. Zeilinger, Dense Coding in Experimental Quantum Communication. *Phys. Rev. Lett.* 76, 4656-4659 (1996).
- [55] Y. Li, Z. Y. Zhou, D. S. Ding, and B. S. Shi, CW pumped telecom band polarization entangled photon pair generation in a Sagnac interferometer. *Opt. Express* 23,28792-28800(2015).
- [56] D. S. Ding, Z. Y. Zhou, B. S. Shi, X. B. Zou, and G. C. Guo, "Generation of non-classical correlated photon pairs via a ladder type atomic configuration: theory and experiment", *Opt. Express* 20, 11433-11444 (2012).
- [57] X. Li, P. L. Voss, J. E. Sharping, and P. Kumar, Optical Fiber Source of Polarization Entangled Photons in the 1550 nm Telecom Band. *Phys. Rev. Lett.* 94, 053601(2004).
- [58] J. Fulconis, O. Alibart, J. L. O'Brien, W. J. Wadsworth, and J. G. Rarity, Non-classical Interference and Entanglement Generation Using a Photonic Crystal Fiber Photon pair Source. *Phys. Rev. Lett.* 99, 120501(2007).
- [59] Richard Chirgwin, Single chip photon source brings quantum comms closer, (2014).

- [60] Fulconis, J., Alibart, O., Wadsworth, W. J. & Rarity, J. G. Quantum interference with photon pairs using two micro-structured fibers. *N. J. Phys.* 9, 276 (2007).
- [61] Muller, A., Fang, W., Lawall, J. & Solomon, G. S. Creating polarization-entangled photon pairs from a semiconductor quantum dot using the optical Stark effect. *Phys. Rev. Lett.* 103, 217402 (2009).
- [62] Scarani, V., de Riedmatten, H., Marcikic, I., Zbinden, H. & Gisin, N. Four-photon correction in two-photon Bell experiments. *Eur. Phys. J. D* 32, 129–138 (2005).
- [63] Christoph Simon, Hugues de Riedmatten, Mikael Afzelius, Nicolas Sangouard, Hugo Zbinden, and Nicolas Gisin. *Phys. Rev. Lett.* 98, 190503 (2007).
- [64] N. Sinclair, E. Saglamyurek, H. Mallahzadeh, J. H. Slater, M. George, R. Ricken, M. P. Hedges, D. Oblak, C. Simon, W. Sohler, and W. Tittel, *Phys. Rev. Lett.* 113, 053603 (2015).
- [65] C. Kurtsiefer, S. Mayer, P. Zarda, and H. Weinfurter, "Stable solid-state source of single photons," *Phys. Rev. Lett.* 85 (2), 290–293 (2000).
- [66] N. Sangouard, C. Simon, J. c. v. Min'ar, H. Zbinden, H. de Riedmatten, and N. Gisin. *Phys. Rev. A* 76, 050301 (2007).
- [67] Nicol o Lo Piparo, William J. Munro, and Kae Nemoto, phoar Xiv:1807.02940v1 [quant-ph] 9 Jul (2018).
- [68] Damien Bonneau , Gabriel J. Mendoza [12] Jeremy L. O, Brien and Mark G, Thompsony , *Phys. Rev.* arXiv:1409.5341v2 [quant-ph] 29 Apr (2015).
- [69] D. Sahin, A. Gaggero, Z. Zhou, S. Jahanmirinejad, F. Mattioli, R. Leoni, J. Beetz, M. Lermer, M. Kamp, S. Höfling, and A. Fiore. Waveguide photon-number-resolving detectors for quantum photonic integrated circuits. *Applied Physics Letters*, 103(11) (2013).

- [70] Marsili F., Verma V. B., Stern J. A., Harrington S., Lita A. E., Gerrits T., Vayshenker I., Baek B., Shaw M. D., Mirin R. P., and Nam S. W. Detecting single infrared photons with 93% system efficiency. *Nat Photon*, 7(3):210–214, 03 (2013).
- [71] Takayuki Kiyohara, Ryo Okamoto, and Shigeki Takeuchi, Vol. 24, No. 24 | 28 Nov | *Optics Express*, 27288, (2016).
- [72] R. Chrapkiewicz and W. Wasilewski, *Opt. Express* 20,29540 (2012).
- [73] S.-Y. Lan, A. G. Radnaev, O. A. Collins, D. N. Matsukevich, T. A. Kennedy, and A. Kuzmich, *Opt. Express* 17,13639(2009).
- [74] A. Grodecka-Grad, E. Zeuthen, and A. S. Sørensen, *Phys. Rev. Lett.* 109, 133601(2012).
- [75] Afzelius, M. Simon, C. De Riedmatten, H. & Gisin, N. Multimode quantum memory based on atomic frequency combs AFC. *Phys. Rev. A* 79, 052329(2009).
- [76] Adrien Nicolas, Thesis De Doctorat del, Universite Pierre et Marie Curie, CH. 1, P 14, (2014).

الخلاصة

إن نقل أي معلومات كمومية عبر مسافات طويلة مع أخطاء أقل هو الهدف الرئيسي لأنظمة الاتصالات الكمية. ولكن ، للأسف ، يتم نقل المعلومات الكمية مباشرة بين أي نقطتين بعيدتين (أليس وبوب) موصولين بالألياف الضوئية محدودة بسبب مشاكل فقدان الفوتون بسبب الانحدار الأسّي لانتقال الضوء بطول الألياف البصرية. لذا ، يقتصر الاتصال الكمي على مسافات قصيرة حيث يمكن الحصول على فك الترابط أثناء النقل بسبب فقدان الفوتون.

ومن ثم ، للتغلب على هذه المسألة ، اقترح Briegel المكرر الكمي في عام 1998 . الهدف الرئيسي من تنفيذ مكرر الكم هو توزيع الفوتونات المتشابكة بين المرسل والمتلقي. مكونات مكرر الكم هي الذاكرة الكمومية ، وقياس حالة بيل ومصادر الفوتون المتشابكة. هناك العديد من مخططات مكرر الكم ، تم اقتراح استخدام بعض مصادر الفوتون الزوج. لكن مصدر زوج الفوتون يعاني من آلية الخطأ المتعلقة بفقدان انبعاث الفوتون بسبب تقليل معدل توزيع الإشارات. لذلك تم استخدام نظام مكرر الكم الآخر في مصدر فوتوني مستخدم واحد وخالي من الخطأ الذي يعاني منه مصدر الفوتون المزدوج ، وبالتالي يمكن تحسين معدل توزيع التشابك.

الأجزاء الأكثر أهمية في مكرر الكم هي الذاكرة الكمومية ومصدر الفوتون المتشابك. في حالة الذاكرة الكمومية ، يتم استخدام الذكريات الكمية متعددة الوسائط ذات زمن عمر قصير في حساباتنا حيث تبين أن الذكريات القصيرة زمن العمر أكثر أهمية في معدل توزيع التشابك الكلي من ذاكرة الكم الطويلة زمن العمر.

وايضا تم هنا اقتراح مخطط مكرر كمي يعتمد على مصدر أزواج الفوتون المضاعف هنا ، وتظهر النتائج تحسناً طفيفاً في معدل توزيع التشابك مقارنة بمخطط مكرر الكوانت استناداً إلى مصدر زوج الفوتون.

على الجانب الآخر ، تم عمل مقارنة حول معدل توزيع التشابك بين مصدر زوج الفوتون ومصدر الفوتون منفرد. واخيرا للحصول على مزيد من التحسينات في توزيع التشابك عبر الاتصالات الكمومية للمسافات الطويلة ، يُقترح هنا أيضاً بنية فعّالة للراغبين الكميّين استناداً إلى مصادر الفوتون منفرد متعددة الإرسال إلى جانب تعدد استخدام ذاكرة كمية متعددة. في هذا العمل ، أجريت دراسة محاكاة باستخدام برنامج محاكاة Python 3.7.



وزارة التعليم العالي والبحث العلمي

جامعة بغداد

معهد الليزر للدراسات العليا

المكررات الكمية المعتمدة على مصدر فوتون منفرد متعدد الارسال

رسالة مقدمة الى

معهد الليزر للدراسات العليا / جامعة بغداد / لاستكمال متطلبات نيل
شهادة ماجستير علوم في الليزر / الهندسة الإلكترونية والاتصالات

من قبل

وجدان محمود خضير

بكالوريوس هندسة الاتصالات - 2007

بإشراف

م. د. جواد عبد الكاظم حسن



وزارة التعليم العالي والبحث العلمي

جامعة بغداد

معهد الليزر للدراسات العليا

المكررات الكمية المعتمد على مصدر فوتون منفرد متعدد الارسال

رسالة مقدمة الى

معهد الليزر للدراسات العليا / جامعة بغداد / لاستكمال متطلبات نيل
شهادة ماجستير علوم في الليزر / الهندسة الإلكترونية والاتصالات

من قبل

وجدان محمود خضير

بكالوريوس هندسة الاتصالات - 2007

بإشراف

م. د. جواد عبد الكاظم حسن